Cell Reports
Medicine

Article

Circadian organization of lipid landscape is perturbed in type 2 diabetic patients

Graphical abstract

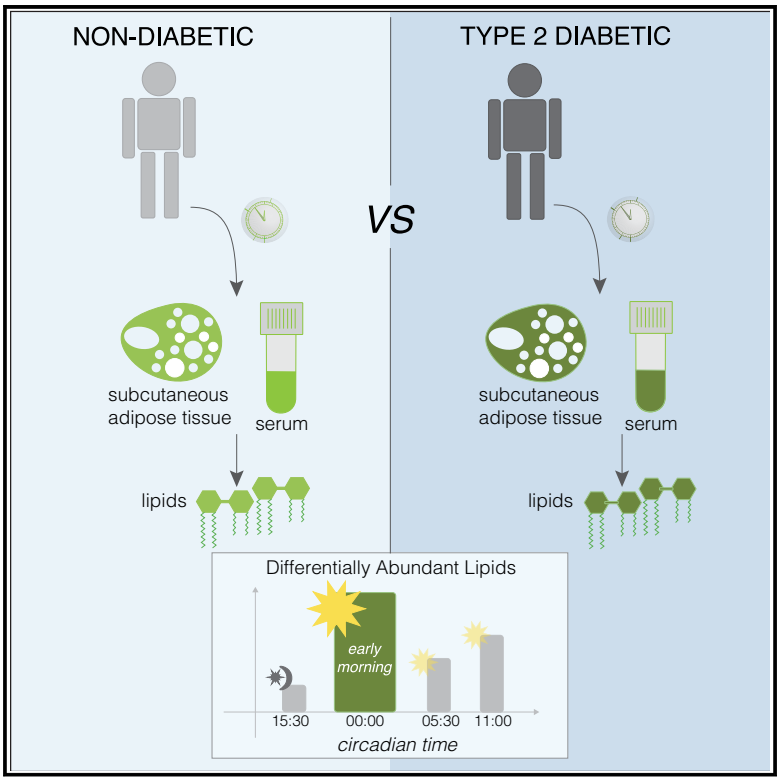

Highlights

- Lipid metabolites exhibit daily rhythms in human serum and white adipose tissue
- The temporal landscape of lipid metabolism is tissue specific and altered in T2D
- Lipids oscillating in both serum and SAT are phase shifted in T2D but not in ND
- The most pronounced differences in serum lipids in T2D are detected early morning

Authors

Flore Sinturel, Simona Chera, Marie-Claude Brulhart-Meynet, ..., Giovanni D'Angelo, Howard Riezman, Charna Dibner

Correspondence

charna.dibner@unige.ch

In brief

Sinturel et al. report that 8% of the lipid metabolites in human serum and subcutaneous adipose tissue follow diurnal rhythmicity. The rhythmic lipidome comparison between non-diabetic and type 2 diabetic (T2D) individuals reveals massive temporal and tissue-specific alterations of the lipid homeostasis in T2D that should be considered in clinics.

Sinturel et al., 2023, Cell Reports Medicine *4*, 101299
December 19, 2023
https://doi.org/10.1016/j.xcrm.2023.101299

CellPress

Cell Reports Medicine

CellPress
OPEN ACCESS

Article

Circadian organization of lipid landscape is perturbed in type 2 diabetic patients

Flore Sinturel,[1,2,3,4] Simona Chera,[1,2,3,4,5] Marie-Claude Brulhart-Meynet,[1,3] Jonathan Paz Montoya,[6] Dirk Jan Stenvers,[7,8] Peter H. Bisschop,[7,8] Andries Kalsbeek,[7,8,9,10] Idris Guessous,[11] François R. Jornayvaz,[2,3,12] Jacques Philippe,[12] Steven A. Brown,[13,15] Giovanni D'Angelo,[6] Howard Riezman,[14] and Charna Dibner[1,2,3,4,16,*]

[1]Division of Thoracic and Endocrine Surgery, Department of Surgery, University Hospitals of Geneva, 1211 Geneva, Switzerland
[2]Department of Cell Physiology and Metabolism, Faculty of Medicine, University of Geneva, 1211 Geneva, Switzerland
[3]Diabetes Center, Faculty of Medicine, University of Geneva, 1211 Geneva, Switzerland
[4]Institute of Genetics and Genomics in Geneva (iGE3), 1211 Geneva, Switzerland
[5]Department of Clinical Science, University of Bergen, 5021 Bergen, Norway
[6]Institute of Bioengineering, School of Life Sciences, EPFL, 1015 Lausanne, Switzerland
[7]Department of Endocrinology and Metabolism, Amsterdam University Medical Centers, University of Amsterdam, Amsterdam, 1105 AZ, the Netherlands
[8]Amsterdam Gastroenterology, Endocrinology and Metabolism (AGEM), Amsterdam University Medical Centers, Amsterdam, 1105 AZ, the Netherlands
[9]Laboratory for Endocrinology, Department of Clinical Chemistry, Amsterdam University Medical Centers, University of Amsterdam, Amsterdam, 1105 AZ, the Netherlands
[10]Netherlands Institute for Neuroscience (NIN), Royal Dutch Academy of Arts and Sciences (KNAW), Amsterdam, 1105 BA, the Netherlands
[11]Department and Division of Primary Care Medicine, University Hospitals of Geneva, 1211 Geneva, Switzerland
[12]Division of Endocrinology, Diabetes, Nutrition, and Therapeutic Patient Education, Department of Medicine, University Hospitals of Geneva, 1211 Geneva, Switzerland
[13]Institute of Pharmacology and Toxicology, University of Zurich, 8057 Zurich, Switzerland
[14]Department of Biochemistry, Faculty of Science, NCCR Chemical Biology, University of Geneva, 1211 Geneva, Switzerland
[15]Deceased
[16]Lead contact
*Correspondence: charna.dibner@unige.ch
https://doi.org/10.1016/j.xcrm.2023.101299

SUMMARY

Lipid homeostasis in humans follows a diurnal pattern in muscle and pancreatic islets, altered upon metabolic dysregulation. We employ tandem and liquid-chromatography mass spectrometry to investigate daily regulation of lipid metabolism in subcutaneous white adipose tissue (SAT) and serum of type 2 diabetic (T2D) and non-diabetic (ND) human volunteers (n = 12). Around 8% of ≈440 lipid metabolites exhibit diurnal rhythmicity in serum and SAT from ND and T2D subjects. The spectrum of rhythmic lipids differs between ND and T2D individuals, with the most substantial changes observed early morning, as confirmed by lipidomics in an independent cohort of ND and T2D subjects (n = 32) conducted at a single morning time point. Strikingly, metabolites identified as daily rhythmic in both serum and SAT from T2D subjects exhibit phase differences. Our study reveals massive temporal and tissue-specific alterations of human lipid homeostasis in T2D, providing essential clues for the development of lipid biomarkers in a temporal manner.

INTRODUCTION

Recent advances in lipidomic approaches have greatly expanded our knowledge regarding the extent and complexity of lipid dysregulation in metabolic diseases. Under homeostatic conditions, the circadian system, comprising a central clock located in the suprachiasmatic nuclei of the hypothalamus and peripheral clocks in the organs, ensures the temporal regulation of the body's metabolism.[1] Peripheral oscillators situated in the liver, muscle, and white adipose tissue function in concert with the central clock to orchestrate glucose, protein and lipid metabolism.[1] Consequently, a significant fraction of the human serum and muscle lipid species exhibits daily rhythmicity.[2–8] The lipid landscape and function are highly tissue-specific at all levels of their activities, including energy storage, cellular membrane organization and signaling.[9] Metabolic disorders such as obesity and type 2 diabetes (T2D) have reached pandemic proportions in modern society characterized by irregular eating patterns, shifted work schedules, and recurring jetlag.[10–12] Emerging evidence indicates a reciprocal connection between altered lipid homeostasis, perturbation of circadian oscillators, and T2D pathology.[13–15] Lipidomic analyses of the human skeletal muscle upon circadian misalignment revealed a significant remodeling of lipid homeostasis,[16] along with a decrease in muscle insulin

sensitivity.[14] Our recent temporal lipidomic profiling of human pancreatic islets derived from non-diabetic (ND) and T2D donors revealed both global and temporal alterations in phospho- and sphingolipids that were associated with decreased cellular membrane fluidity in T2D islets and compromised insulin secretion.[15] At present, deep circadian lipidome profiling of metabolically active tissues is scarce. Considering the tight interaction between circadian rhythm and lipid metabolism, identification of tissue- and time-specific lipid signatures is urgently required. Here, we investigated the temporal profiles of a wide spectrum of serum and subcutaneous white adipose tissue (SAT) lipid metabolites in T2D patients and ND controls by using tandem mass spectrometry (MS) and liquid chromatography (LC) MS lipidomic in two human cohorts. Our study reveals that the global lipid landscape exhibits significant temporal variations on a daily basis in a tissue-specific manner, and provides temporal lipid metabolite signatures in T2D serum and SAT.

RESULTS

Glycerophospholipid and ceramide levels are altered in the serum of cohort 1 T2D patients

Two groups of six participants each were enrolled in the human cohort 1: lean ND (control group) and overweight or obese T2D men (T2D group). For details of human cohort 1, see Figure 1A, Table S1, the STAR Methods section, and Stenvers et al.[17] Serum lipidomics analyses identified 444 lipid metabolites across major lipid classes: phosphatidylethanolamines (PE), phosphatidylcholines (PC), phosphatidylinositols (PI), cardiolipins, ceramides (Cer), and hexosylceramides (HexCer) (Table S2). We first compared the lipid levels averaged across four time points between the control and T2D subjects (Figures 1B–1G and S1A–S1F). Hierarchical clustering analysis of the top 50 altered lipid metabolites demonstrated a clear separation of the samples collected from T2D and control donors (Figure 1B). Overall, PI and PE lipids, particularly the diacyl ones, were increased in T2D patient sera, concomitant with a decrease in PCs and CLs (Figures 1B, 1C, 1E–1G, S1B, and S1C). No significant changes in the overall amount of metabolites per lipid class were observed between the groups (Figure 1D). However, the total amount of ether PCs (PC(O-)) has been decreased in the T2D group (Figure 1F). Among the upregulated diacyl PE lipids in T2D, we noticed the increase in all unsaturated PE sub-species, with the difference in polyunsaturated (PUFA) 2-PE reaching statistical significance (Figure S1B). CLs showed an overall decrease in the T2D group, with all CLs exhibiting lower levels compared with the control group, regardless of their carbon chain length (Figure S1C). Cers were increased in the T2D group, while the levels of the HexCers remained comparable in both groups (Figures 1B, 1C, and S1D–S1F).

Temporal profiling of the human serum reveals the most pronounced differences in the lipid context between T2D and ND controls at the wake-up (ZT0:00) time

We next analyzed the temporal alterations in serum lipid levels at the four consecutive time points across 24 h (Figure 2A). Lipid changes were strongly associated with a collection time point, revealing time-dependent signatures for several lipid classes (Table 1, cohort 1). Indeed, alterations in the sphingolipids and lysoPCs in the serum of T2D and control subjects have solely been measured at ZT0:00 (Figures 2B–2F). Notably, most of the downregulated serum PC lipids at ZT11:00 were ether, rather than lysoPC, metabolites, as shown by the significant decrease of this PC subclass in T2D individuals compared with the control counterparts (Figures S2A and S2B). While alterations in PEs have only been recorded at ZT11:00 (Figures S2A and S2C), most of the significantly decreased CLs in the T2D group were measured at ZT05:30, and to a lesser extent at ZT11:00 (Figures S2A and S2D).

A high variation in the number of differentially abundant lipids (DALs) between the two groups has been observed at different times of the day (Figure 2A). Most striking differences were detected at the wake-up time of the participants (ZT0:00, between 6:30 a.m. and 8:00 a.m., Table S1), with 49 DALs reported at ZT0:00 compared with 7 at ZT15:30 (Figures 2B, 2C, and S2E). Furthermore, the principal component analysis (PCA) conducted at ZT0:00 demonstrated a better separation between the two groups of subjects, as compared with the PCA analysis conducted on the lipid levels averaged across all time points (Figures S1A; and S2F).

Serum lipidome signature that distinguishes T2D subjects is similar in two independent human cohorts

We next focused on lipid homeostasis alterations upon T2D in serum of the cohort 1 participants at the early morning time point ZT0:00 that exhibited the most pronounced changes between the groups. We have recently conducted lipid landscape analyses at a single morning time point in serum of T2D and ND individuals in a larger human cohort, employing the same methodology for the lipid measurements (cohort 2; n = 16 per group) (Table S3 and Methods[18]). In the cohort 2 study, blood samples were collected between 8 and 10 a.m., following overnight fasting, which roughly corresponds with ZT0:00 in cohort 1. We thus re-analyzed the lipidomic data from sera obtained from cohort 2 individuals (Table S4) to cross-compare our novel data from cohort 1 with a similar subset of samples conducted on independent cohort 2. For both datasets related to cohorts 1 and 2, we conducted a differential analysis of lipid abundance and hierarchical clustering (Figures 2B, 2C, and 2G–2H). Overall, the alterations in the T2D serum lipidome in both cohorts followed similar trends, which were characterized by a decrease in several lysoPCs and PEs and an increase in PIs (Figures 2B–2D and 2G–2H). A high number of Cers, dihydroceramides (DHCer) and hexosyldihydroceramides (HexDHCer) were upregulated in the T2D group of the cohort 1, resulting in a trend for a total DHCer increase and significant upregulation of the total HexDHCer levels (Figures 2B–2F). Similarly, we report an upregulation of sphingolipids in the cohort 2 T2D group, notably of DeoxCers that were only analyzed in this cohort (Figure 2H). Due to the larger size of the cohort 2 compared with cohort 1, the differences observed in cohort 2 reached higher significance (Figures 2B and 2H). Noteworthy, while cohort 1 is only composed of male subjects, the cohort 2 is balanced regarding the sex of the participants (Tables S1 and S3). A comparison between the lipid context in the samples obtained from male and female sub-cohorts of the cohort 2 revealed striking differences (Figure S3). Indeed, we report

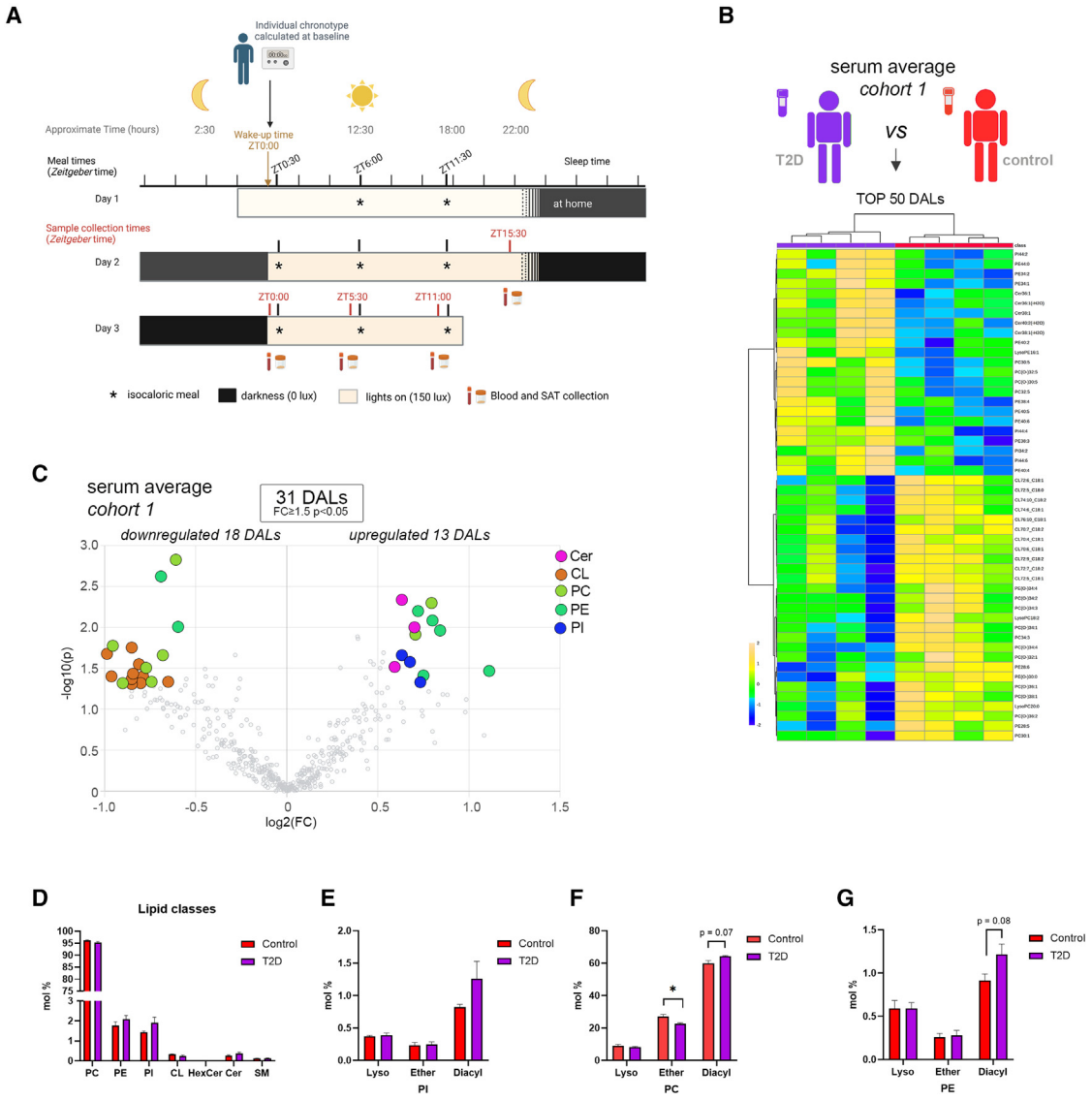

Figure 1. Serum lipidome from T2D and control donors

(A) Study design summary. Asterisks indicate the hourly intake meals. Sampling times are indicated in red and represented by blood and tissue vials.

(B) Hierarchical clustering analysis of top 50 serum lipids with most contrasting patterns between T2D and control subjects.

(C) Volcano plot of the DALs between T2D and control donors. Colored dots highlight significant up- or down-regulated individual lipids (fold change ≥ 1.5 and $p < 0.05$, Welch's corrected).

(D) Lipid class repartition in serum from control ND and T2D donors (mol %).

(E–G) Relative serum PI (E), PC (F), and PE (G) levels (mol %) in T2D and control donors. Lipids are clustered according to the nature of the fatty acid linkage (diacyl vs. alkyl-acyl [ether] or monoacyl [lyso]). Statistics for (D–G) are unpaired t tests with Welch's correction. For (B–D), lipid levels measured across time points were averaged. Data for T2D and control subjects (n = 4 per group) are represented as mean ± SEM. *p < 0.05. See also Figure S1.

substantial variations in the lipid classes and number of lipid metabolites that were differently abundant between T2D and control samples in males versus females (Figure S3). When male sub-cohort of the cohort 2 was compared with the cohort 1, the upregulation of Cers and HexCers in the T2D group was fully recapitulated (Figures 2B, 2C, S3A, and S3B). In contrast, DeoxCers were significantly enriched in the sera of the T2D female sub-cohort 2 compared with their control counterparts (Figures S3C and S3D), suggesting that T2D-associated lipidomic fingerprints in the serum are sex-dependent.

Temporal analyses of SAT lipidome highlight elevated PI and DHCer levels in T2D subjects, with the most pronounced differences at ZT05:45

We next examined the lipid landscape in SAT collected from T2D and control subjects at 4 time points across 24 h (Table S5),

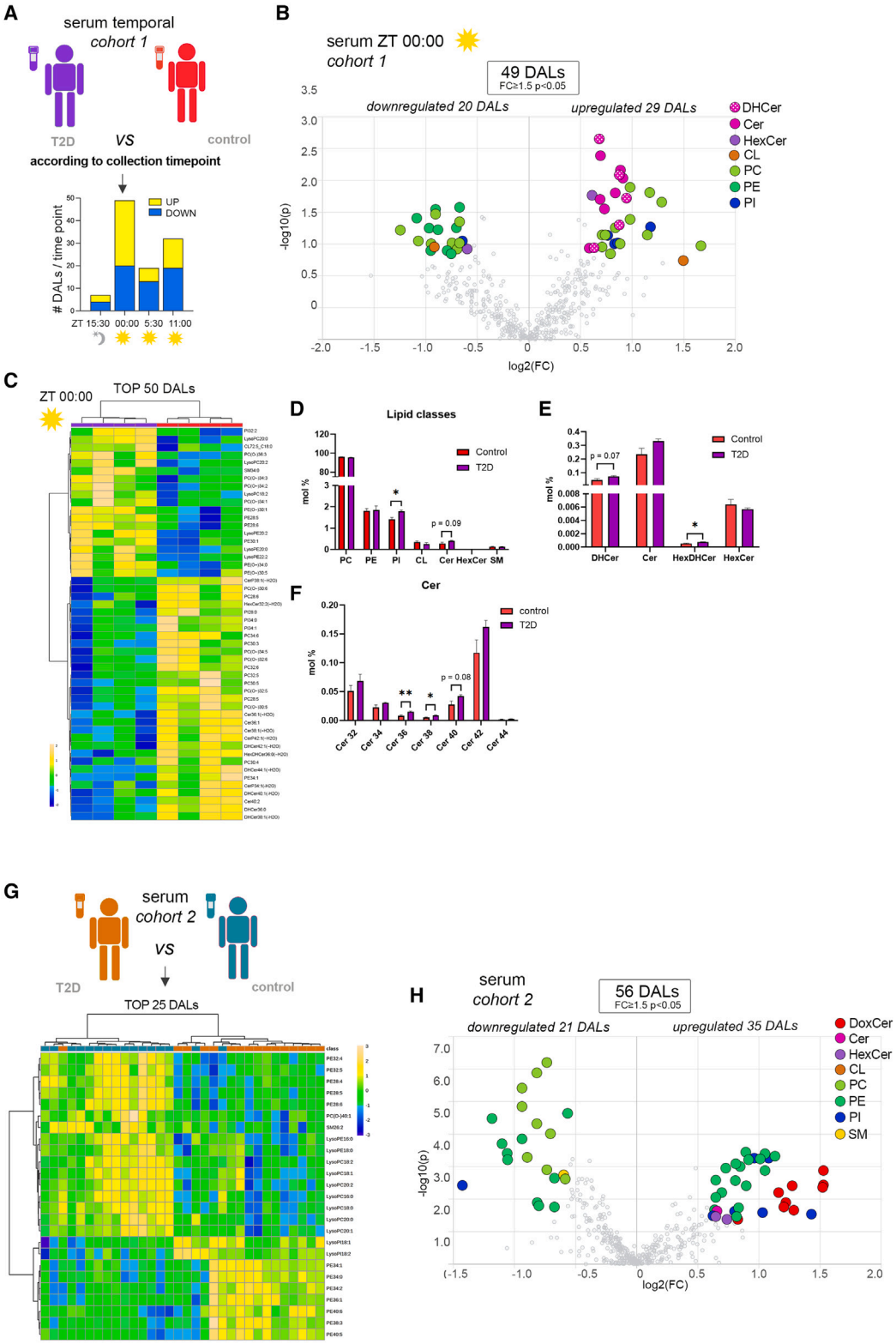

(legend on next page)

Table 1. Time-specific alterations in major lipid classes upon T2D in serum and SAT

	Time points				
	ZT15:30	ZT0:00		ZT05:30	ZT11:00
Tissue	cohort 1	cohort 1	cohort 2	cohort 1	cohort 1
Serum		↑ PI ↑ DHCer ↑ HexDHCer ↓ LysoPC	↑ PI ↑ DeoxCer ↓ LysoPC	↓ CL	↑ PE ↑ Diacyl PC ↓ CL ↓ Ether PC
SAT	↑ PI	↑ PI ↑ DHCer ↓LysoPC		↑ Lyso/Ether PI ↑ DHCer ↑ HexCer ↑Long-chain PUFA TAGs	↑ Ether PI ↑ DeoxCer ↓ PE

Up and down arrows indicate increased and decreased levels, respectively.

mirroring the blood sampling. Similar to the averaged serum lipid analyses (Figures 1B–1G and S1A–S1F), comparison of the SAT lipids averaged across the time points did not reveal significant changes in overall amounts per lipid class (Figures S4A–S4D). The number of DALs was lower in SAT compared with sera (Figures 1B, 1C, 3A, and 3B). Out of all DAL, a large fraction (17/22) was upregulated, while only a minor fraction (5) was downregulated. Concomitant decrease of PCs and increase in several PIs and DHCers was observed in T2D participants compared with the controls (Figures 3A–3D and S4C). Interestingly, we noticed a trend to decrease in the PUFA-PEs content in the T2D SAT, along with an elevated PC/PE ratio (Figures S4E and S4F).

Of note, the observed lipid alterations were consistent with the altered mRNA levels encoding for the key enzymes of lipid metabolism that we previously measured on SAT samples from cohort 1.[17] Indeed, *AGPAT9* and the ceramidase *ACER2* were downregulated in the T2D SAT (Figures S4G and S4H), in an agreement with the decreased levels of Lyso- and diacyl-PCs and increased amounts of DHCers observed in the same samples (Figures 3C and 3D). Similarly, *PEMT* encoding for the key enzyme in the PE to PC conversion was upregulated in T2D samples (Figure S4I), in an agreement with the observed altered PC/PE ratio in the diseased samples (Figure S4F).

Similar to the serum analyses, temporal analysis of the SAT DALs at individual time points detected highly time-dependent lipid signatures (Figures 3E and 3F; Table 1). The highest number of DALs was measured at ZT05:45, corresponding with midday, and the lowest at ZT15:30, just before bedtime (Figures 3F and S4J). The tendency for upregulation of PIs and DHCers has been observed in T2D samples across most of time points (Figures 3F and S4J–S4N), with the overall amount of DHCers being significantly upregulated at ZT05:45 only (Figure S4K). The total amount of PIs was upregulated in the T2D group, with ether lipid family showing the most significant upregulation (Figures S4J, S4M, and S4N). Additionally, HexDHCers were upregulated at ZT05:45 (Figure S4K), whereas several PCs showed increased levels at ZT00:15 (Figure 3F). Among the downregulated species at ZT11:15, a majority belonged to PEs, along with few PI and PC species (Figures 3F and S4J).

Identification of daily rhythmic lipid metabolites in serum and SAT

To investigate the diurnal rhythmicity of lipid metabolites in human serum and SAT, we analyzed the temporal profiles of the lipids identified at the four time points. Strikingly, the overall amount of metabolites exhibited comparable temporal patterns in serum and SAT, with a nadir around ZT0:00 (Figures 4A and 4B). Temporal lipid profiles from control and T2D individuals largely overlapped, although control serum lipids showed a greater amplitude of diurnal variations compared with those from the T2D counterpart (Figure 4A). To assess whether the observed diurnal variations of lipid metabolites qualified as daily rhythmic, we applied two algorithms used for circadian rhythm detection that allow to analyze unevenly time-distributed samples: Lomb-Scargle (LS) periodogram[19] and CosinorJ.[20] Whereas CosinorJ has been developed for rhythmic analyses of serial samples with low and possibly uneven temporal resolution[20] and

Figure 2. Temporal variations in the serum lipidome from T2D and control donors

(A) Around-the-clock analysis of the serum DALs between T2D and control donors conducted separately in each time point.

(B) Volcano plot of the serum DALs collected at ZT00:00 between T2D and control donors.

(C) Hierarchical clustering analysis of top 50 serum lipids with most contrasting patterns between T2D and control subjects at ZT00:00.

(D) Lipid class repartition in sera collected at time point ZT00:00 from control and T2D donors (mol %).

(E) Relative levels (mol %) of DHCer, Cer, HexDHCer, and HexCer in sera collected at ZT00:00 from T2D and control donors.

(F) Relative Cer levels (mol %) in sera collected at ZT00:00 from T2D and control donors, represented according to the chain length.

(G) Hierarchical clustering analysis of top 25 serum lipids with most contrasting patterns between T2D and controls (n = 16 per group) from cohort 2. Sera were collected between 8:00 a.m. and 10:00 a.m.

(H) Volcano plot of the serum DALs collected between 8:00 a.m. and 10:00 a.m. from cohort 2 T2D and control subjects (n = 16 per group). Statistics for (D–F) are unpaired t tests with Welch's correction. For the panels (A–F), data are represented as mean ± SEM. *p < 0.05 (n = 4 per group). For the volcano plots (B, H), colored dots highlight significant up- or down-regulated individual lipids (fold change ≥1.5 and p < 0.05, Welch's corrected). See also Figures S2 and S3.

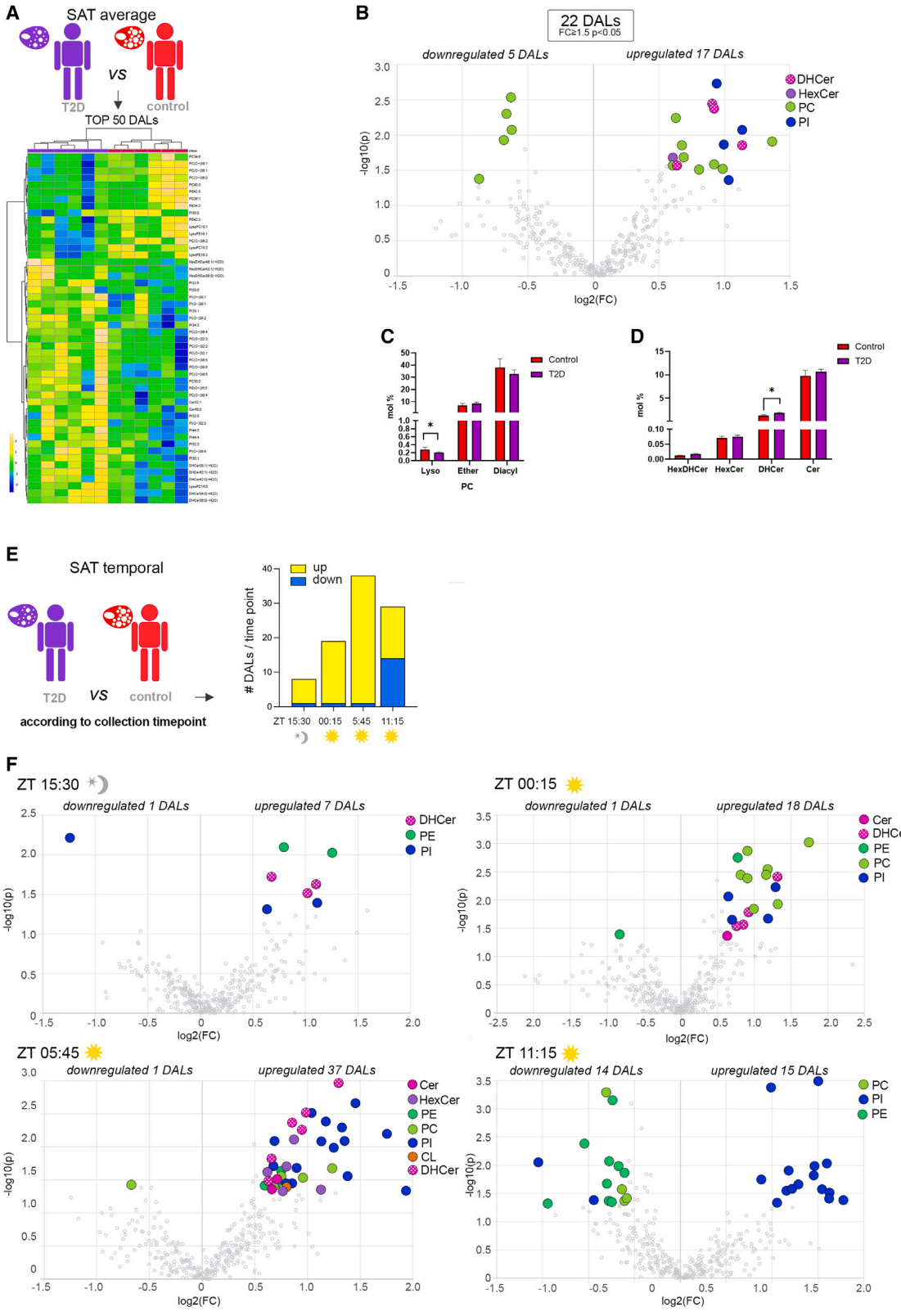

(legend on next page)

is thus mostly appropriate for the presented here dataset analyses, LS is a very stringent algorithm that is in principle suboptimal for qualifying circadian rhythmicity in datasets with low time resolution.[21] Indeed, while CosinorJ alone qualified a large portion of lipids as daily rhythmic (13%–40% depending on the tissue and participant), LS detected no significantly rhythmic species in our datasets (Table S6). We thus selected the top 50 lipid metabolites with the lowest p values obtained by the LS analyses. Venn analyses combining both algorithms (Figure 4C) allowed to select the lipids that were both significantly rhythmic according to CosinorJ and had the lowest p values based on the LS algorithm. The resulting commonly identified metabolites were qualified daily rhythmic (STAR Methods) (Figure 4C and Table S6). Based on the combined LS and CosinorJ analyses, we calculated the percentage of oscillating lipids per tissue and per group of participants. On average, we detected a slightly higher percentage of oscillating lipids in SAT (≈8.5%) compared with the serum (≈7.5%) for both groups (Figures 4D and S5A–S5D). The distribution of rhythmic lipids indicated that certain lipid classes were preferentially subjected to daily oscillations (Figures S5A–S5D). In serum, PEs, PIs, CLs, and the sphingolipids were particularly enriched with rhythmic species in both groups, although the cyclic PE species were less represented in T2D (Figures S5A and S5C). In SAT, a large number of sphingolipids qualified as rhythmic, with some differences between the T2D and controls (Figures S5B and S5D). Indeed, looking at the repartition of the rhythmic lipids within their corresponding lipid class, we observed that the SM contained a higher percentage of oscillating lipids in both T2D SAT and serum (Figure 4E). In contrast, the fraction of oscillating HexCers differed between the subject groups and tissues, with a higher percentage of rhythmic HexCers observed in the control SAT (Figure 4E). Furthermore, averaged temporal profiles largely varied across the lipid classes, depending on both tissue and study group (Figures S5E–S5H). Noteworthy, the most abundant phospholipids (PC, PE, and PI) exhibited a clear tendency to peak around ZT11:00-15:30 and decrease at ZT0:00 across study groups and tissues, except for the control SAT (Figures S5E–S5H).

HexCer lipids show diurnal accumulation in ND individuals

Zooming into the diurnal lipid variations in each tissue and group of donors independently, we observed a significant diurnal profile of the average HexCer lipids in the control sera (Figure 4F). The temporal profiles of individual HexCer exhibited high variability, with the HexCers C30, C34, and C42 qualified as daily rhythmic (Figure 4G). In the control group, ether phospholipids exhibited rhythmicity, with ether PE sub-class being significantly rhythmic (Figure 4H), and PI(O-)38:1 oscillating in the serum of three of the four subjects (Figure 4I). Turning to the SAT, although the average HexCer profile did not qualify as significantly rhythmic (Figure S5G), abundant HexCer metabolites C32 and C42 (Figure S4D) qualified as oscillating in the control group (Figure 4J), similar to the trend observed in serum. Temporal profiles of SAT PCs varied depending on their saturation degree, with monounsaturated fatty acid (MUFA) and PUFA 3-PC metabolites accumulating in a diurnal manner reaching a peak at ZT05:45 (Figure 4K).

In T2D subjects, the diurnal lipid signature is tissue specific

The spectrum of rhythmic lipid classes differed between T2D and control groups. In T2D individuals, PE lipids exhibited comparable temporal profiles in serum and SAT, regardless of their degree of saturation (Figures S5I and S5J). In T2D SAT, the daily accumulation of PCs and PEs was comparable (Figures 4K and S5J). Notably, the PUFA/MUFA ratio significantly oscillated throughout the day for PCs and PEs (Figure 4L). In the serum, the overall temporal accumulation of SMs showed a daily rhythm, with the majority of SMs peaking at ZT0:00 as exemplified by SM44:0 (Figures 4M and 4N). Similarly, we observed a significant enrichment of some ceramides in the sera collected at ZT0:00 (Figure 4O). In summary, SM and Cer lipids showed daily rhythms in serum but not in T2S SAT, whereas PCs and PEs exhibited similar temporal variations in the two tissues.

The differences in diurnal phase of PC and PE lipids between T2D and control individuals are influenced by their degree of saturation

The temporal analyses conducted separately for each tissue and study group revealed that PEs, and to a lesser extent PCs, were oscillating under several conditions (Figures S5E–S5J). Strikingly, daily rhythmic profiles of PC and PE lipids reached their maximal levels at different time points in the serum and SAT of control donors (Figures 5A, S5I, and S5J). In contrast, the PC and PE temporal profiles largely overlapped between T2D serum and SAT (Figure 5B). Major differences between control and T2D groups were observed depending on the lipid saturation degree. Indeed, MUFA and PUFA 3-PC were significantly rhythmic in T2D and control SAT; however, their oscillation peaks were strongly shifted between T2D and controls (Figure 5C). Similarly, the rhythmicity of the PE lipids varied depending on the saturation degree and the donor group. In serum, saturated fatty acyl (SFA) and MUFA-PE exhibited comparable temporal profiles

Figure 3. Temporal variations in the SAT lipidome from T2D and control donors

(A) Hierarchical clustering analysis of top 50 SAT lipids with most contrasting patterns between T2D and control subjects.

(B) Volcano plot of the DALs between T2D and control SAT.

(C) Relative PC levels (mol %) in T2D and control SAT. Lipids are clustered according to the nature of the fatty acid linkage (diacyl vs. alkyl-acyl [ether] or monoacyl [lyso]).

(D) Relative levels (mol %) of DHCer, Cer, HexDHCer, and HexCer in T2D and control SAT.

(E) Analysis of the SAT DALs between T2D and control at the four time points.

(F) Volcano plot of the DALs between T2D and control SAT at the indicated time points. Data for (A–D) represent the average across time points. Data for (C and D) are presented as mean ± SEM and statistics are unpaired t test with Welch's correction. *$p < 0.05$. For the volcano plots (B and F), colored dots highlight significant up- or down-regulated individual lipids (fold change ≥1.5 and $p < 0.05$, Welch's corrected). See also Figure S4.

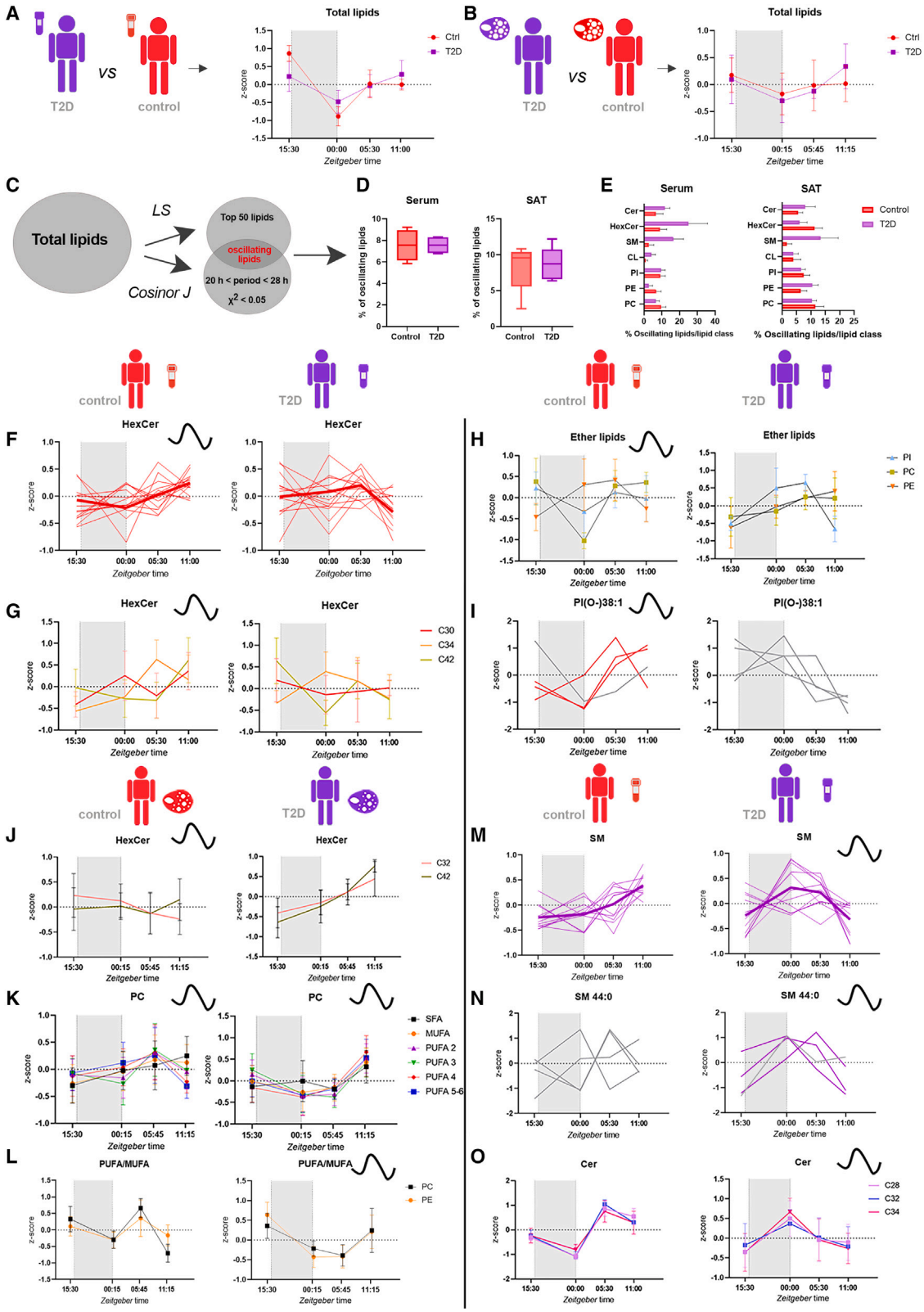

(legend on next page)

(except at ZT11:00) in T2D and controls, although SFA-PE showed significant daily rhythms for the control group only, and the MUFA-PE for the T2D group (Figures 5D and S5I). In contrast, PUFA 2-3-PE peaks were shifted between the control and T2D SAT samples, with a maximal enrichment at ZT05:45 and between ZT11:15 and 15:30, respectively (Figure 5E).

Key enzymes of lipid metabolism exhibit diurnal mRNA expression profiles in SAT samples that are altered in T2D

Importantly, the diurnal transcriptome study conducted by us previously on SAT samples from cohort 1 revealed that a subset of genes, including those related to adipogenesis, was qualified as diurnal rhythmic in the control subjects, but lost their rhythmicity in T2D.[17] Thus, the expression profile of *ACER2* that exhibited diurnal rhythmicity in control SAT biopsies was flattened (Figure S4H) and overall diminished in T2D counterpart (Figure S5K). Furthermore, *AGPAT2*, a key enzyme in the *de novo* biosynthesis of all phospholipids, as well as the fatty acid elongase *ELOVL5*, involved in the synthesis of long-chain MUFA and PUFA, exhibited rhythmic gene expression in the control SAT with the trough around ZT0:00 (Figures S5L–S5M). Furthermore, the rhythmic profile of *AGPAT2* in the control SAT corroborated the temporal variations of the total lipids measured in our study (Figure 4B). The rhythmicity of *AGPAT2* expression was attenuated in the SAT from T2D subjects (Figures S5G–S5H). *ELOVL5*, which was also identified as daily rhythmic in human skeletal muscle biopsies from ND subjects,[3] acts specifically toward PUFA acyl-CoA.[22,23] Thus, the diurnal changes in the expression of this enzyme may account for the temporal phase differences of the PUFA PE and PC lipids observed upon T2D (Figures 4K, 5C, 5E, and S5J). Overall, the reported rhythmicity of the genes encoding for the key enzymes of the lipid biosynthesis and its alterations upon T2D may corroborate, at least in part, the observed lipid changes.

In T2D subjects, the lipids exhibiting diurnal rhythmicity in both serum and SAT display phase differences between the tissues

To further examine the concordance between the rhythmic metabolites in serum and SAT, we analyzed the daily lipid profiles in both tissues separately for each subject (Figures 5F and 5G). The number of common rhythmic lipids was low for both T2D and control individuals, ranging from 0 to 4. Due to inter-individual variability, none of these lipids was common across all the subjects. Noteworthy, most of the metabolites exhibited comparable temporal profiles in serum and SAT for the control group, except for HexCer38:2(-H_2O) (Figure 5H). In contrast, only SM44:2 displayed overlapping diurnal patterns in serum and SAT from the T2D individuals, whereas most of the other common rhythmic lipid metabolites showed shifted oscillation peak timings (Figure 5I). Thus, in contrast with control individuals, most of the common rhythmic lipids identified in T2D subjects exhibited oscillating patterns that were strongly phase shifted between serum and SAT.

Absolute levels and temporal profiles of DeoxCers are altered in SAT of T2D individuals

In agreement with our previous lipidomic study conducted at a single time point,[18] the data presented here highlight the specific abundance of several DHCer-H_2O species in serum and especially in SAT upon T2D (Figures 2B, 2C, 2H, 3A, 3B, and 3D–3F). Given that the DHCer-H_2O metabolites have the same *m/z* ratio as the non-canonical 1-deoxyceramides (DeoxCer) that we previously identified in large amount in human visceral adipose tissue collected from obese T2D patients,[18] we next looked closer at the abundance and the temporal accumulation of DeoxCers in the SAT of the cohort 1 participants by LC-MS (Figure 6A and Table S7). When the measurements conducted at four time points were averaged, we detected a trend for increased DeoxCer levels in T2D SAT (Figure 6A). Two-way

Figure 4. Identification of rhythmic lipids in SAT and serum from control and T2D participants

(A and B) Average temporal levels of total lipids in serum (A) and SAT (B) from control and T2D individuals.

(C) Schematic representation of the rhythmic analysis workflow. Lipids were considered oscillating when they were identified among the top 50 most rhythmic lipids according to LS algorithm, and exhibited a significant oscillation by CosinorJ.

(D) Average percentage of oscillating lipids in serum (left) and SAT (right) from control and T2D groups. Whiskers represent the minimum and maximum values.

(E) Representation of the rhythmic lipid/lipid class percentage of serum (left) and SAT (right) lipids in control and T2D subjects.

(F) Temporal levels of HexCers measured in sera. Red bold trace corresponds to the *Z* score value of the average profile of HexCer lipids, identified as daily rhythmic.

(G and H) Average temporal levels of three HexCers (G) and ether PIs, PCs, and PEs (H) measured in control sera. HexCer C30, C34, C42, and ether PI were qualified as rhythmic.

(I) Representative example of an ether lipid temporal profile: PI(O-)38:1 identified as rhythmic in three control sera. Colored traces correspond with the donors exhibiting a diurnal profile of PI(O-)38:1.

(J) Average temporal levels of two rhythmic HexCer lipids measured in SAT.

(K) Average temporal profiles of PCs measured in the SAT of control individuals and sorted by degree of unsaturation, from SFA to PUFA lipids. MUFA and PUFA-3 profiles were identified as daily rhythmic.

(L) Average temporal profiles of PC and PE PUFA/MUFA ratio, where both PC and PE were identified as daily rhythmic in SAT.

(M) Temporal levels of all SMs measured in the T2D sera. Bold trace corresponds with the *Z* score value of the average profile of all the SM lipids qualified rhythmic.

(N) Representative example of an SM temporal profile: SM44:0 qualified rhythmic in three T2D sera. Colored traces correspond with the donors exhibiting a rhythmic profile of SM44:0.

(O) Average temporal profiles of three rhythmic Cers clustered by chain length and measured in T2D sera. Data for (A, B, E, G, H, J, L, and O) are presented as mean ± SEM. Lipid temporal profiles (A, B, and F–O) are represented as normalized *Z* score values; for (F and M), values were normalized to the lipid mean value per individual analysis and then averaged across all subjects for each time point. For serum n = 4, for SAT samples n = 6 subjects per group. Sinusoid signs indicate the graphs where at least one lipid or lipid class is qualified rhythmic. See also Figure S5 and Table S6 for statistical values of the rhythmic lipids.

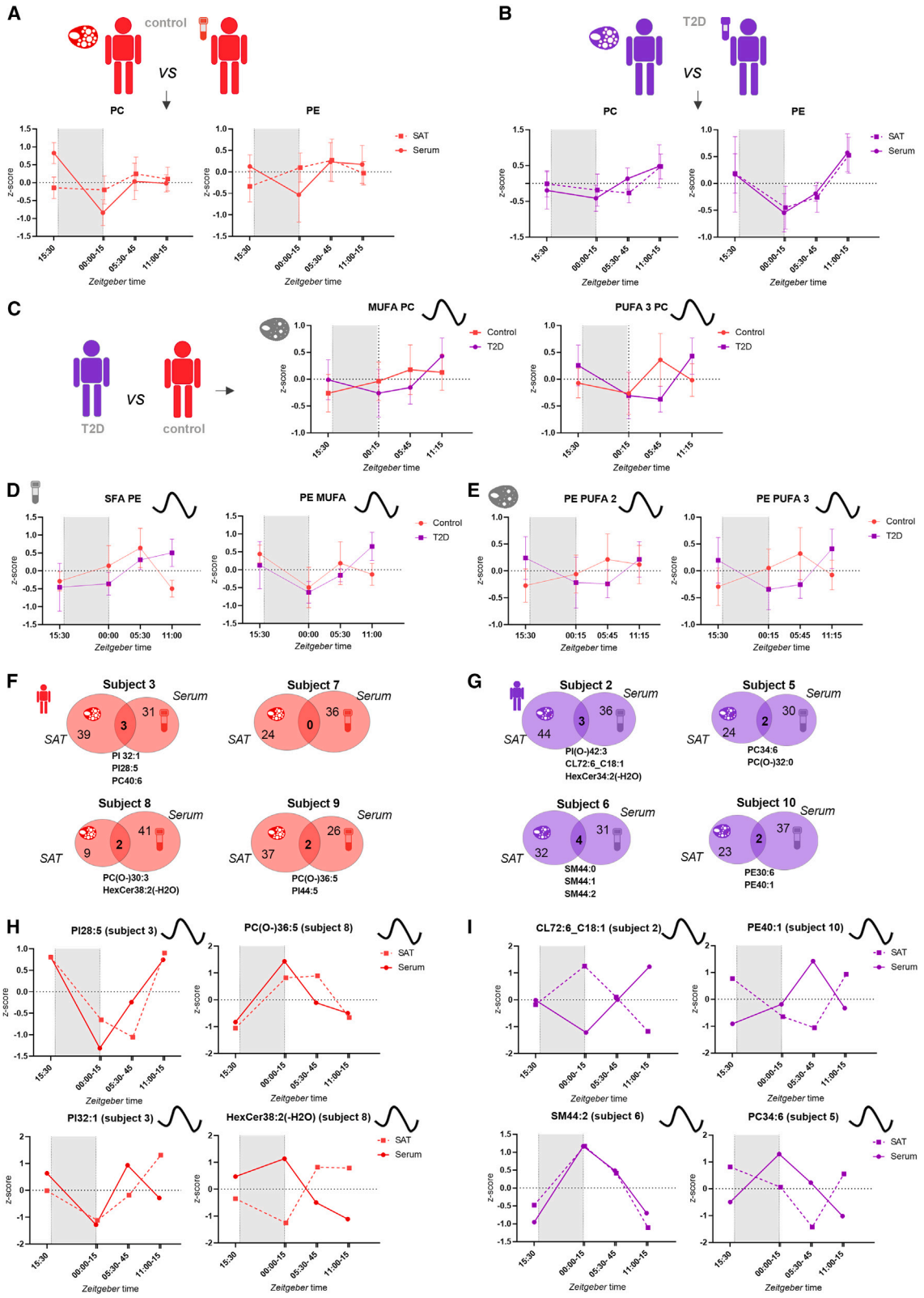

(legend on next page)

ANOVA revealed a significant interaction effect between time of day and T2D disease, suggesting a differential temporal regulation of DeoxCer lipid abundance between the T2D and control SAT (Figure 6B). We observed the most striking differences in the evening (ZT11:15), where nearly all DeoxCers were more abundant in the T2D SAT compared with the controls. This difference reached significance for some DeoxCer species (Figures 6C and 6D). Surprisingly, we also noticed a slight decrease of DeoxCer levels in the T2D samples compared with controls at ZT00:15 and 05:45 (Figures 6D and 6E). In fact, these variations resulted from strongly phase-shifted temporal patterns of DeoxCer accumulation in the two groups of participants (Figure 6E). Circadian analysis of the individual DeoxCers in each group revealed four species with significant daily rhythmicity in the T2D SAT, and one in the control counterpart (Figures 6F and 6G).

Global and temporal alterations of TAG and DAG levels in SAT of T2D individuals are associated with their degree of saturation

TAGs are very abundant glycerolipids in human SAT,[24] with their accumulation being considered a hallmark of obesity. Some TAG metabolites, in particular those carrying long-chain PUFAs,[5] were previously identified as daily rhythmic in human blood plasma, and to a lesser extent in human skeletal muscle biopsies.[2,3] Employing LC-MS, we measured TAG and DAG levels in the neutral fraction of the lipid extracts from SAT biopsies collected around the clock (Tables S8 and S9). When averaged across all time points, comparable amounts of total TAGs have been observed in the two study groups (Figure 6H). Interestingly, the PUFA 6-TAG levels were significantly increased in the T2D SAT across all the time points, with marked differences for the long-chain TAG_56 (Figures 6I–6K). When analyzed at four consecutive time points, PUFA 6- and 7-TAGs were identified as daily rhythmic in the control group, but not in the SAT of the T2D participants (Figure 6L). Overall temporal profiles of TAGs did not qualify as significantly rhythmic, likely due to the strong amplitude and peak time variations on a per-individual basis (Figure 6M).

Compared with TAGs, DAGs are present in smaller quantities in the human SAT.[24] We observed a comparable abundance of overall DAGs control and T2D groups (Figure 6N), similar to TAG lipids (Figure 6H). While only few individual DAG metabolites showed significant changes upon T2D (DAGs 31:0 and 30:2), hierarchical clustering analysis of the top five modified DAGs allowed for clear discrimination between the samples collected from T2D and control donors (Figure 6O). These five DAGs that exhibited lower levels in T2D individuals bore 0 to 2 double bonds, suggesting a lower abundance of saturated DAGs. The DAG levels did not follow significant rhythmic daily changes either in the control or in the T2D groups (Figure 6P). When analyzed separately, saturated DAGs showed significant daily rhythms in the control SAT (Figure 6Q) that was lost in the T2D (Figure 6Q).

DISCUSSION

There is emerging evidence that, in a physiological context, the lipid landscape is subject to diurnal variations in human serum,[5,25] in the skeletal muscle,[2,3] and in pancreatic islets synchronized *in vitro*.[15] Here we demonstrate that also in SAT, a fraction of lipid metabolites undergo daily rhythms. Around 8% of all lipid metabolites across major lipid classes exhibited diurnal oscillations in SAT, suggesting a widespread rhythmic control of lipid pathways in this metabolically active tissue. A similar fraction of lipids bearing significant daily rhythms was observed in the sera obtained at the same time points from the same participants. A spectrum of daily oscillating lipids displayed a striking difference between serum and SAT (Figures 4A–4E and S5A–S5D). In ND individuals, a previous circadian lipidomic study conducted in ''constant routine'' conditions across 28 h, reported a slightly higher number of oscillating species (13%) in the serum.[5] This discrepancy might be explained by differences in the time resolution, cohort size, the number of measured lipids, and different algorithms applied to assess the lipid rhythmicity. Noteworthy, the study by Chua and colleagues showed that lipid oscillatory profiles were highly heterogeneous among the 20 individual subjects analyzed, whereas core body temperature, salivary melatonin, and plasma cortisol were comparable across participants.[5] Similar variability regarding individual lipid oscillations has been previously observed by us in human skeletal muscle, along with comparable circadian phase of core-clock transcripts in the same muscle biopsies.[3] Here, we report substantial variations in the number and type of rhythmic lipid species identified among the individuals in the control group, despite the standardization of the food intake and sleep/wake schedules (Figures 4D, 4E, and 5F). The broad distribution of lipid oscillatory profiles among human individuals in serum is in good agreement with previous works.[3,5,6,26] Thus, our lipidomic profiling further highlights the existence of distinct circadian metabolic phenotypes in SAT across human individuals. While the origin of individual lipid rhythms remains to be

Figure 5. Comparison of SAT and serum rhythmic lipid temporal profiles in control and T2D participants

(A and B) Average temporal levels of total PCs (left) and PEs (right) in serum and SAT samples collected from control (A) and T2D (B) individuals.

(C) Comparison of MUFA-PC (left) and PUFA 3-PC (right) average temporal profiles of control and T2D SAT qualified rhythmic in both groups. See also Figures 4L and 4Q.

(D) Comparison of average temporal profiles of serum SFA-PE (left, qualified rhythmic in control) and MUFA-PE (right, qualified rhythmic in T2D).

(E) Comparison of PUFA 2-PE (left) and PUFA 3-PE (right) average temporal profiles measured in control and T2D SAT (PUFA-2 PE was qualified rhythmic in control, and PUFA 3-PE in T2D).

(F and G) Identification of lipids commonly rhythmic in both serum and SAT in the four subjects, either control (F) or T2D (G). Venn diagram represents the number of the significantly rhythmic metabolites identified in serum, in SAT, and in both, for each participant.

(H and I) Representative examples of lipid profiles identified as rhythmic in both serum and SAT in control (H) and T2D (I) individuals. Data for (A–E, H, and I) e represented as normalized *Z* score values, mean ± SEM. For serum samples n = 4; for SAT n = 6 subjects per group. Sinusoid signs indicate the graphs where at least one lipid or lipid class is qualified rhythmic. See also Figure S5 and Table S6 for statistical values of the rhythmic lipids.

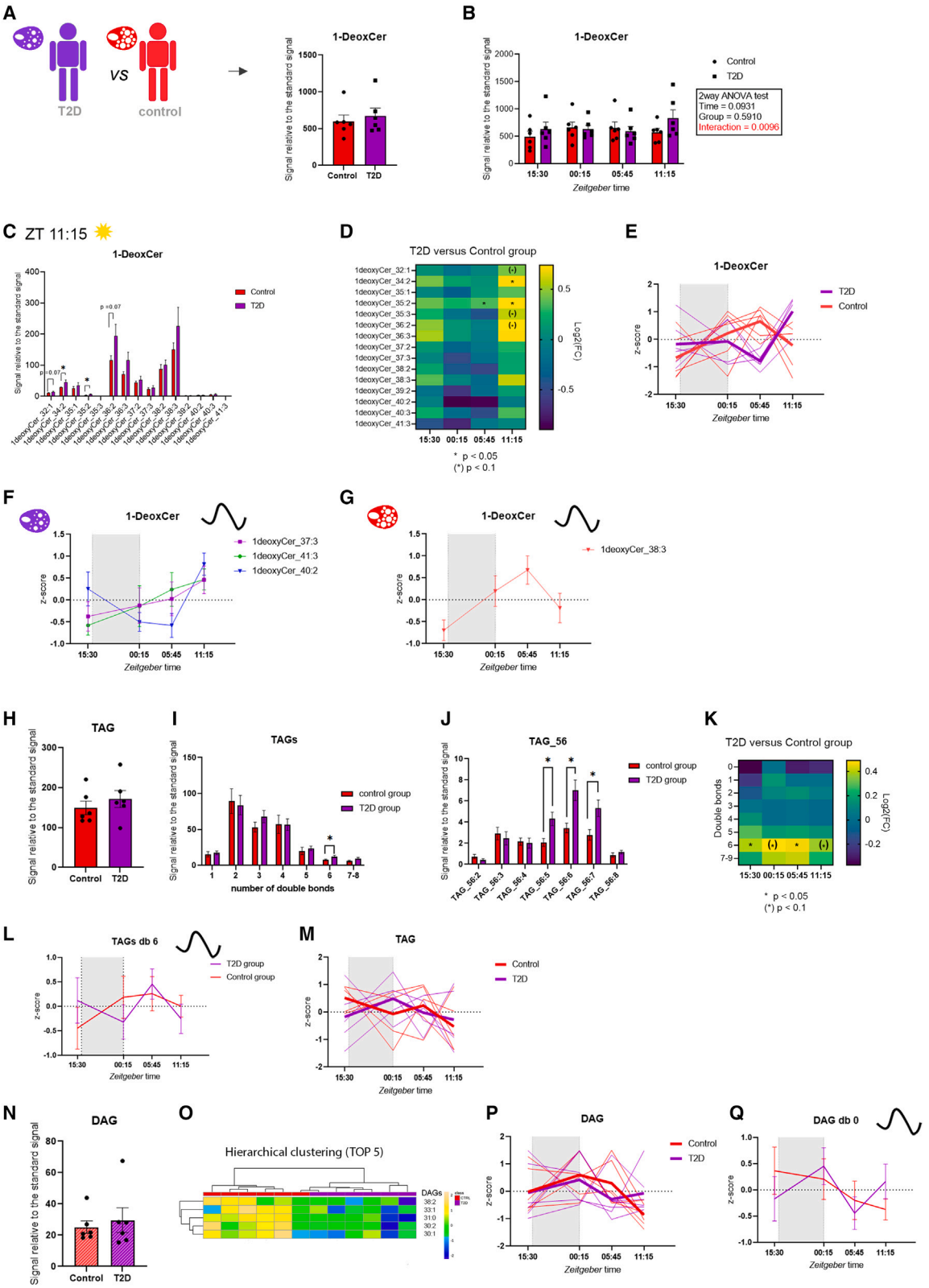

(legend on next page)

explored, the existence of temporal-, tissue-, and person-specific metabolic phenotypes must be taken into account in future human studies of lipid homeostasis.

In our work, overall serum and SAT lipids exhibited comparable patterns of accumulation across 24 h with a peak at ZT15:30 (Figures 4A and 4B). Among the measured lipid metabolites, HexCers and ether phospholipids represented the most significant daily oscillating serum lipids (Figures 4F–4I). In agreement with Chua et al., who described a small number of sera plasmalogen PCs as group rhythmic,[5] we observed a peak concentration of these lipids in the evening (Figure 4H). In SAT, we discovered that HexCers, representing a minor fraction of lipids (Figure S4B), encompassed a high number of rhythmic species (Figures 4E and S5B). In previous works, HexCers were reported to be rhythmic in synchronized human pancreatic islets[15] and in human skeletal muscle biopsies, albeit to a lesser extent.[2,3] TAGs and DAGs exhibited milder rhythmicity in SAT, with a peak during evening and morning hours, respectively (Figures 6M and 6P), in agreement with the timing of plasma TAG rhythms reported upon constant routine.[6] Of note, TAGs were strongly rhythmic in the serum of ND subjects and exhibited a morning peak,[5] further highlighting the tissue specificity of the lipid rhythmicity.

Turning to the comparison of lipid signatures between control and T2D subjects, we report global changes in glycerophospholipids that were either specific for serum or SAT, or shared among the two (Figures 1B, 1C, 3A, and 3B). One common denominator of average lipid landscape across 24 h in both serum and SAT in T2D subjects is the increase in some PI species (Figures 1B, 1C, 3A, and 3B). Altered PI metabolism has already been proposed to take part in the development of insulin resistance in rodents.[27,28] Our work reveals significantly increased accumulation of PIs upon T2D in serum and SAT, promoting the idea that these lipids may contribute to the pathophysiology of T2D in humans. Notably, some alterations in the balance of lipid species upon T2D were observed exclusively in serum or in SAT, highlighting that lipid signatures associated with the pathogenesis of T2D are tissue-specific. Regarding the serum only, the most striking differences between control and T2D subjects encompassed a trend in diacyl PC and PE increase, along with a significant decrease in PC(O-) in the T2D group (Figures 1B, 1C, 1F–1G, and S1B).

LysoPCs, among other lysophospholipids, represent signaling molecules that act through G-protein-coupled receptors and are involved in multiple pathways. Previous studies reported diminution of LysoPC levels in plasma and skeletal muscle in the context of obesity/overweight-associated T2D.[18,29–34] Our study demonstrates that, also in SAT of T2D patients, the levels of LysoPC lipids were decreased (Figure 3C). In view of raised potential of LysoPC metabolites as biomarkers for T2D risk,[35,36] exploring mechanistic insights into the roles of LysoPC lipids in the pathogenesis of T2D development represents an important perspective for future studies.[35,36]

DHCers represent an additional group of lipids that has been proposed as potential biomarkers for T2D.[37] In this study, we report a significant increase of DHCers in the SAT of T2D patients (Figure 3D). In cohort 2, we reported that some DeoxCer metabolite levels were elevated in serum of T2D patients (Figures 2G and 2H), consistent with other works.[18,38,39] Along the same lines, our LC-MS analysis conducted in the SAT of cohort 1 showed a tendency for a global DeoxCer increase in T2D subjects (Figure 6A). DeoxCers are considered cytotoxic; they cannot be converted to complex sphingolipids or degraded by the canonical degradation pathway.[40–42] Thus, elevated levels of DeoxCers observed during the development of T2D are likely to contribute to the pathophysiology, although the mechanisms underlying such cytotoxicity remain unclear.

Beyond the absolute changes, our study of the lipid temporal profiles in control and T2D subjects revealed that both the

Figure 6. SAT 1-deoxyceramides exhibit differential absolute and temporal levels in control and T2D individuals

(A) LC-MS signals for DeoxCer levels in SAT collected from T2D and control donors. For each donor, total DeoxCers measured across four time points were averaged. The difference is not statistically significant.

(B) Temporal comparison of DeoxCer levels at four consecutive time points from T2D and control donors. The result of the two-way ANOVA test is indicated in the figure.

(C) LC-MS signals for DeoxCer measured at ZT11:15 from T2D and control subjects, showing significant abundance of DeoxCer with short chain length in T2D.

(D) Heatmap of DeoxCer log2-transformed fold changes between control versus T2D at each time point.

(E) Temporal levels of total DeoxCer for each subject (T2D, control). Bold traces correspond to the average profile of all participants in each group, not significantly rhythmic.

(F and G) Average temporal profiles of the DeoxCers qualified rhythmic in control (F) and T2D (G). In the control group, 1-deoxyCer_38:3 was qualified rhythmic, and 1-deoxyCer_41:3, 1-deoxyCer_37:3, and 1-deoxyCer_40:2 in the T2D.

(H) LC-MS signals for TAG levels in T2D and control SAT.

(I) LC-MS signals for individual TAGs sorted by number of double bonds and measured in T2D and control SAT.

(J) LC-MS signals for TAG:56 species sorted by number of double bonds and measured in T2D and control subjects.

(K) Heatmap of TAGs sorted by number of double bonds, log2-transformed fold changes between control versus T2D individuals at each time point.

(L) Average temporal profiles of the TAG lipids bearing six double bonds in T2D and control. The profile was qualified rhythmic in the control.

(M) Temporal total TAG levels for each subject. Bold traces correspond to the average profile across all the participants in each group.

(N) LC-MS signals for DAG levels in T2D and control.

(O) Hierarchical clustering analysis of top 5 DAGs with most contrasting patterns between T2D and control subjects.

(P) Temporal total DAG levels for each subject. Bold traces correspond with the average profile across all the participants in each group.

(Q) Average temporal profiles of the DAGs bearing 0 double bond in T2D and control. The profile was qualified rhythmic in the control group. Data for (A–C, F–J, L, N, and Q) are presented as mean ± SEM. Lipid temporal profiles (E–G, L, M, P, and Q) are presented as normalized *Z* score values. Data for (A, H–J, N, and O) represent the average of total lipids measured across four time points for each donor. Statistics for (A, C, D, and H–K) are unpaired Student's t tests with Welch's correction p values (n = 6 per group). (*) $p < 0.1$, *$p < 0.05$. Sinusoid signs indicate the graphs where at least one lipid or lipid class is qualified rhythmic. See also Table S6 for statistical values of the rhythmic lipids.

spectrum of the lipid metabolites and their rhythmicity were altered in T2D. Remarkable differences have been identified between the profiles of several lipid classes and lipid metabolites, accounting for the variations observed in the number of lipids differentially abundant at each time point (Figures 2A and 3E). Recent work comparing the temporal distribution of metabolites conducted in lean, obese, and T2D men demonstrated a differential pattern of metabolite class distribution across the time points and between the study groups.[34] Recently, temporal comparison of the muscle metabolome in young healthy and older metabolically compromised men showed the greatest differences between groups at 4 a.m.[26] Concordantly, we report the most substantial changes in serum lipids between the T2D and control groups at early morning time point, following the over-night fasting. Given that eating represents a potent clock synchronizer, one can assume that overnight fasting preceding the morning blood sampling contributes to the maximum of lipid differences observed at this time point between the groups.

One striking example of specific temporal changes upon T2D is the DeoxCer group. Whereas global changes in DeoxCer lipids did not reach statistical significance in T2D SAT (Figure 6A), a significant increase in several DeoxCer species has been observed at ZT11:15 (Figures 6C and Table 1). Indeed, a temporal analysis of DeoxCer abundance revealed strong diurnal differences in the accumulation of the DeoxCers and phase-shifted profiles of these lipids between the control and T2D groups (Figure 6E). These pronounced temporal differences likely account for the lack of significant changes that we observe for lipid metabolite values averaged across the four time points.

Of note, the circadian transcriptome study conducted by us previously on SAT samples from cohort 1 showed attenuated rhythmicity of core-clock gene expression in SAT from T2D individuals compared with control counterparts.[17] Furthermore, temporal profiles of adipogenesis regulators *ACER2*, *AGPAT2*, and *ELOVL5* were robustly rhythmic in the ND but not in T2D samples (Figures S5K–S5M). Additionally, the expression of the phosphatidate phosphatase *PPAP2*, essential for the synthesis of glycerolipids, and of *PEMT* (Figure S4I), which converts PE to PC, were upregulated at all time points in the T2D group. This change may explain the phospholipid level alterations, along with the trend for higher PC/PE ratio upon T2D (Figures 3A, 3B, and S4F). Similarly, RNA expression of *AGPAT9*, the key enzyme in *de novo* synthesis of lysophosphatidic acid,[43] whose activity is enhanced by insulin stimulation,[44,45] was downregulated in the SAT of T2D subjects (Figure S4G). It is thus plausible to hypothesize that circadian regulation of the rhythmic lipid landscape might be mediated, at least in part, via the rhythmic regulation of the key enzymes of the lipid metabolism, like it has been previously reported for the circadian regulation of various metabolic pathways.[8]

Our study demonstrates that, in a physiological context, the global lipid landscape is a subject to significant temporal alterations in SAT and serum on a daily basis. This notion is extremely important to consider for the human studies of lipid homeostasis in metabolic diseases. Moreover, it may explain discrepancies in the identification of lipid metabolites associated with T2D in studies conducted at one time point only, that do not take into account the time dimension of lipid homeostasis.[18,29–31,35,37,46,47] Indeed, our findings highlight that, due to the differences in temporal alterations in the lipid landscape that were lipid class-, disease-, organ-, and patient sex-specific, it is essential to identify the time point across 24 h that corresponds with the most pronounced difference for a given lipid metabolite between the study groups. Taking into consideration the circadian rhythmicity of lipid metabolism will ensure the correct implementation of newly identified lipid biomarkers for the development of metabolic diseases. Last, it is of utmost clinical importance to unravel whether the alterations in the temporal lipid landscape could be restored via targeting the circadian clock machinery, for instance, by using small clock modulator molecules[48] or lifestyle adaptations,[8] or otherwise via bariatric surgery, in cases where important metabolic decompensation cannot be readily reversed by lifestyle adaptations alone.[49]

Limitations of the study

Several factors limit the interpretation of our experiments. First, cohort 1 encompasses a low number of subjects along with low temporal resolution. Due to the relatively invasive character of repetitive ventral SAT biopsies, it is generally difficult to ensure the enrollment of a larger human cohort with more frequent SAT sampling. A low number of participants and large inter-individual differences within the study groups in terms of circadian phase of lipid oscillations impinged on the quality of statistical analyses. Therefore, statistical significance qualifying the comparison between the two groups must be taken with caution. Furthermore, the T2D group participants were treated with metformin and/or other glucose-lowering drugs (Tables S1 and S3), whereas the subjects from the control group did not receive these medications. Thus, we cannot formally exclude a bias in our analyses stemming from chronic medication administration. Additionally, the low temporal resolution rendered proper evaluation of statistical significance for the circadian profiles somewhat limited. To cope with this limitation, we combined the two most advanced analysis tools generally used in the circadian field, LS and CosinorJ. Finally, recent lipidomic data reported sex-specific associations among the lipid species associated with obesity,[50] in a good agreement with our own findings (Figure S3). Since our cohort 1 is only composed of male subjects, not allowing to extrapolate the conclusions to both sexes, conducting a similar temporal lipid profiling in female participants would be necessary.

STAR★METHODS

Detailed methods are provided in the online version of this paper and include the following:

- KEY RESOURCES TABLE
- RESOURCE AVAILABILITY
  - Lead contact
  - Materials availability
  - Data and code availability
- EXPERIMENTAL MODEL AND STUDY PARTICIPANT DETAILS
  - Study design and patient characteristics
- METHOD DETAILS

- Study design, blood and tissue sampling
- Blood measurements
- Materials for lipid extraction
- Serum lipid extraction procedure
- SAT lipid extraction procedure
- Determination of total phosphorus
- Phospho- and sphingolipid analysis by MS
- TAG, DAG and Deoxysphingolipid analysis by LC-MS

- QUANTIFICATION AND STATISTICAL ANALYSIS
- ADDITIONAL RESOURCES

SUPPLEMENTAL INFORMATION

Supplemental information can be found online at https://doi.org/10.1016/j.xcrm.2023.101299.

ACKNOWLEDGMENTS

We are deeply saddened by the tragic death of our outstandingly valued colleague and dear friend Steven A. Brown, who made essential contribution to this study.

We thank Thomas J. Hannich for his constructive comments on the lipidomic analyses.

This work was supported by grant 310030_184708/1, the Vontobel Foundation, the Novartis Consumer Health Foundation, EFSD/Novo Nordisk Programme for Diabetes Research in Europe, Swiss Life Foundation, the Olga Mayenfisch Foundation, the Fondation pour l'innovation sur le cancer et la biologie, Ligue Pulmonaire Genevoise, Swiss Cancer League, Velux Foundation, Leenaards Foundation, ISREC Foundation, and the Gertrude von Meissner Foundation (C.D.); by Young Independent Investigator Grant SGED/SSED and Swiss Life Foundation (F.S.); by the Research Council of Norway 314397 (S.C.); and by ZonMW Agiko stipend 92003592 (D.J.S.).

AUTHOR CONTRIBUTIONS

F.S. performed lipidomics experiments; F.S. and S.C. performed the data analyses; M.C.B.M. and J.P.M. assisted with the lipidomics; D.J.S., P.H.B., and A.K. conceptualized the cohort 1 study and provided the samples; C.D., I.G., F.R.J., J.P., and S.A.B. conceptualized the cohort 2 study; G.d.A. and H.R. contributed to the lipidomics conceptualization; F.S. and C.D. drafted the manuscript; F.S. and C.D. have unrestricted access to all data; all authors agreed to submit the manuscript, read and approved the final draft, and take full responsibility of its content, including the accuracy of the data and the fidelity of the trial to the registered protocol and its statistical analysis.

DECLARATION OF INTERESTS

The authors declare no competing interests.

INCLUSION AND DIVERSITY

While citing references scientifically relevant for this work, we also actively worked to promote gender balance in our reference list.

Received: December 20, 2022
Revised: June 26, 2023
Accepted: October 30, 2023
Published: November 27, 2023

REFERENCES

1. Sinturel, F., Petrenko, V., and Dibner, C. (2020). Circadian Clocks Make Metabolism Run. J. Mol. Biol. *432*, 3680–3699.
2. Held, N.M., Wefers, J., van Weeghel, M., Daemen, S., Hansen, J., Vaz, F.M., van Moorsel, D., Hesselink, M.K.C., Houtkooper, R.H., and Schrauwen, P. (2020). Skeletal muscle in healthy humans exhibits a day-night rhythm in lipid metabolism. Mol. Metabol. *37*, 100989.
3. Loizides-Mangold, U., Perrin, L., Vandereycken, B., Betts, J.A., Walhin, J.P., Templeman, I., Chanon, S., Weger, B.D., Durand, C., Robert, M., et al. (2017). Lipidomics reveals diurnal lipid oscillations in human skeletal muscle persisting in cellular myotubes cultured in vitro. Proc. Natl. Acad. Sci. USA *114*, 8565–8574.
4. Chua, E.C.P., Shui, G., Cazenave-Gassiot, A., Wenk, M.R., and Gooley, J.J. (2015). Changes in Plasma Lipids during Exposure to Total Sleep Deprivation. Sleep *38*, 1683–1691.
5. Chua, E.C.P., Shui, G., Lee, I.T.G., Lau, P., Tan, L.C., Yeo, S.C., Lam, B.D., Bulchand, S., Summers, S.A., Puvanendran, K., et al. (2013). Extensive diversity in circadian regulation of plasma lipids and evidence for different circadian metabolic phenotypes in humans. Proc. Natl. Acad. Sci. USA *110*, 14468–14473.
6. Kent, B.A., Rahman, S.A., St Hilaire, M.A., Grant, L.K., Rüger, M., Czeisler, C.A., and Lockley, S.W. (2022). Circadian lipid and hepatic protein rhythms shift with a phase response curve different than melatonin. Nat. Commun. *13*, 681.
7. Kyle, J.E., Bramer, L.M., Claborne, D., Stratton, K.G., Bloodsworth, K.J., Teeguarden, J.G., Gaddameedhi, S., Metz, T.O., and Van Dongen, H.P.A. (2022). Simulated Night-Shift Schedule Disrupts the Plasma Lipidome and Reveals Early Markers of Cardiovascular Disease Risk. Nat. Sci. Sleep *14*, 981–994.
8. Petrenko, V., Sinturel, F., Riezman, H., and Dibner, C. (2023). Lipid metabolism around the body clocks. Prog. Lipid Res. *91*, 101235.
9. Furse, S., Fernandez-Twinn, D.S., Jenkins, B., Meek, C.L., Williams, H.E.L., Smith, G.C.S., Charnock-Jones, D.S., Ozanne, S.E., and Koulman, A. (2020). A high-throughput platform for detailed lipidomic analysis of a range of mouse and human tissues. Anal. Bioanal. Chem. *412*, 2851–2862.
10. Vetter, C., Devore, E.E., Ramin, C.A., Speizer, F.E., Willett, W.C., and Schernhammer, E.S. (2015). Mismatch of Sleep and Work Timing and Risk of Type 2 Diabetes. Diabetes Care *38*, 1707–1713.
11. Nowak, N., Rawleigh, A., and Brown, S.A. (2021). Circadian Clocks, Sleep, and Metabolism. Adv. Exp. Med. Biol. *1344*, 21–42.
12. Parameswaran, G., and Ray, D.W. (2022). Sleep, circadian rhythms, and type 2 diabetes mellitus. Clin. Endocrinol. *96*, 12–20.
13. Kessler, K., Gerl, M.J., Hornemann, S., Damm, M., Klose, C., Petzke, K.J., Kemper, M., Weber, D., Rudovich, N., Grune, T., et al. (2020). Shotgun Lipidomics Discovered Diurnal Regulation of Lipid Metabolism Linked to Insulin Sensitivity in Nondiabetic Men. J. Clin. Endocrinol. Metab. *105*, dgz176.
14. Wefers, J., van Moorsel, D., Hansen, J., Connell, N.J., Havekes, B., Hoeks, J., van Marken Lichtenbelt, W.D., Duez, H., Phielix, E., Kalsbeek, A., et al. (2018). Circadian misalignment induces fatty acid metabolism gene profiles and compromises insulin sensitivity in human skeletal muscle. Proc. Natl. Acad. Sci. USA *115*, 7789–7794.
15. Petrenko, V., Sinturel, F., Loizides-Mangold, U., Montoya, J.P., Chera, S., Riezman, H., and Dibner, C. (2022). Type 2 diabetes disrupts circadian orchestration of lipid metabolism and membrane fluidity in human pancreatic islets. PLoS Biol. *20*, e3001725.
16. Harmsen, J.F., van Polanen, N., van Weeghel, M., Wefers, J., Hoeks, J., Vaz, F.M., Pras-Raves, M.L., van Kampen, A.H.C., Schaart, G., van Moorsel, D., et al. (2021). Circadian misalignment disturbs the skeletal muscle lipidome in healthy young men. Faseb. J. *35*, e21611.
17. Stenvers, D.J., Jongejan, A., Atiqi, S., Vreijling, J.P., Limonard, E.J., Endert, E., Baas, F., Moerland, P.D., Fliers, E., Kalsbeek, A., and Bisschop, P.H. (2019). Diurnal rhythms in the white adipose tissue transcriptome are disturbed in obese individuals with type 2 diabetes compared with lean control individuals. Diabetologia *62*, 704–716.
18. Hannich, J.T., Loizides-Mangold, U., Sinturel, F., Harayama, T., Vandereycken, B., Saini, C., Gosselin, P., Brulhart-Meynet, M.C., Robert, M., Chanon, S., et al. (2021). Ether lipids, sphingolipids and toxic

1-deoxyceramides as hallmarks for lean and obese type 2 diabetic patients. Acta Physiol. *232*, e13610.

19. Glynn, E.F., Chen, J., and Mushegian, A.R. (2006). Detecting periodic patterns in unevenly spaced gene expression time series using Lomb-Scargle periodograms. Bioinformatics *22*, 310–316.
20. Mannic, T., Meyer, P., Triponez, F., Pusztaszeri, M., Le Martelot, G., Mariani, O., Schmitter, D., Sage, D., Philippe, J., and Dibner, C. (2013). Circadian clock characteristics are altered in human thyroid malignant nodules. J. Clin. Endocrinol. Metab. *98*, 4446–4456.
21. Mei, W., Jiang, Z., Chen, Y., Chen, L., Sancar, A., and Jiang, Y. (2021). Genome-wide circadian rhythm detection methods: systematic evaluations and practical guidelines. Briefings Bioinf. *22*, bbaa135.
22. Leonard, A.E., Bobik, E.G., Dorado, J., Kroeger, P.E., Chuang, L.T., Thurmond, J.M., Parker-Barnes, J.M., Das, T., Huang, Y.S., and Mukerji, P. (2000). Cloning of a human cDNA encoding a novel enzyme involved in the elongation of long-chain polyunsaturated fatty acids. Biochem. J. *350 Pt 3*, 765–770.
23. Ohno, Y., Suto, S., Yamanaka, M., Mizutani, Y., Mitsutake, S., Igarashi, Y., Sassa, T., and Kihara, A. (2010). ELOVL1 production of C24 acyl-CoAs is linked to C24 sphingolipid synthesis. Proc. Natl. Acad. Sci. USA *107*, 18439–18444.
24. Lange, M., Angelidou, G., Ni, Z., Criscuolo, A., Schiller, J., Blüher, M., and Fedorova, M. (2021). AdipoAtlas: A reference lipidome for human white adipose tissue. Cell Rep. Med. *2*, 100407.
25. Davies, S.K., Ang, J.E., Revell, V.L., Holmes, B., Mann, A., Robertson, F.P., Cui, N., Middleton, B., Ackermann, K., Kayser, M., et al. (2014). Effect of sleep deprivation on the human metabolome. Proc. Natl. Acad. Sci. USA *111*, 10761–10766.
26. Harmsen, J.F., van Weeghel, M., Parsons, R., Janssens, G.E., Wefers, J., van Moorsel, D., Hansen, J., Hoeks, J., Hesselink, M.K.C., Houtkooper, R.H., and Schrauwen, P. (2022). Divergent remodeling of the skeletal muscle metabolome over 24 h between young, healthy men and older, metabolically compromised men. Cell Rep. *41*, 111786.
27. Nagao, M., Esguerra, J.L.S., Asai, A., Ofori, J.K., Edlund, A., Wendt, A., Sugihara, H., Wollheim, C.B., Oikawa, S., and Eliasson, L. (2020). Potential Protection Against Type 2 Diabetes in Obesity Through Lower CD36 Expression and Improved Exocytosis in β-Cells. Diabetes *69*, 1193–1205.
28. Manna, P., and Jain, S.K. (2012). Decreased hepatic phosphatidylinositol-3,4,5-triphosphate (PIP3) levels and impaired glucose homeostasis in type 1 and type 2 diabetic rats. Cell. Physiol. Biochem. *30*, 1363–1370.
29. Yin, X., Willinger, C.M., Keefe, J., Liu, J., Fernández-Ortiz, A., Ibáñez, B., Peñalvo, J., Adourian, A., Chen, G., Corella, D., et al. (2020). Lipidomic profiling identifies signatures of metabolic risk. EBioMedicine *51*, 102520.
30. Razquin, C., Toledo, E., Clish, C.B., Ruiz-Canela, M., Dennis, C., Corella, D., Papandreou, C., Ros, E., Estruch, R., Guasch-Ferré, M., et al. (2018). Plasma Lipidomic Profiling and Risk of Type 2 Diabetes in the PREDIMED Trial. Diabetes Care *41*, 2617–2624.
31. Floegel, A., Stefan, N., Yu, Z., Mühlenbruch, K., Drogan, D., Joost, H.G., Fritsche, A., Häring, H.U., Hrabě de Angelis, M., Peters, A., et al. (2013). Identification of serum metabolites associated with risk of type 2 diabetes using a targeted metabolomic approach. Diabetes *62*, 639–648.
32. Tonks, K.T., Coster, A.C., Christopher, M.J., Chaudhuri, R., Xu, A., Gagnon-Bartsch, J., Chisholm, D.J., James, D.E., Meikle, P.J., Greenfield, J.R., and Samocha-Bonet, D. (2016). Skeletal muscle and plasma lipidomic signatures of insulin resistance and overweight/obesity in humans. Obesity *24*, 908–916.
33. Barber, M.N., Risis, S., Yang, C., Meikle, P.J., Staples, M., Febbraio, M.A., and Bruce, C.R. (2012). Plasma lysophosphatidylcholine levels are reduced in obesity and type 2 diabetes. PLoS One *7*, e41456.
34. Isherwood, C.M., Van der Veen, D.R., Johnston, J.D., and Skene, D.J. (2017). Twenty-four-hour rhythmicity of circulating metabolites: effect of body mass and type 2 diabetes. Faseb. J. *31*, 5557–5567.
35. Suvitaival, T., Bondia-Pons, I., Yetukuri, L., Pöhö, P., Nolan, J.J., Hyötyläinen, T., Kuusisto, J., and Orešič, M. (2018). Lipidome as a predictive tool in progression to type 2 diabetes in Finnish men. Metabolism *78*, 1–12.
36. Wang-Sattler, R., Yu, Z., Herder, C., Messias, A.C., Floegel, A., He, Y., Heim, K., Campillos, M., Holzapfel, C., Thorand, B., et al. (2012). Novel biomarkers for pre-diabetes identified by metabolomics. Mol. Syst. Biol. *8*, 615.
37. Wigger, L., Cruciani-Guglielmacci, C., Nicolas, A., Denom, J., Fernandez, N., Fumeron, F., Marques-Vidal, P., Ktorza, A., Kramer, W., Schulte, A., et al. (2017). Plasma Dihydroceramides Are Diabetes Susceptibility Biomarker Candidates in Mice and Humans. Cell Rep. *18*, 2269–2279.
38. Bertea, M., Rütti, M.F., Othman, A., Marti-Jaun, J., Hersberger, M., von Eckardstein, A., and Hornemann, T. (2010). Deoxysphingoid bases as plasma markers in diabetes mellitus. Lipids Health Dis. *9*, 84.
39. Othman, A., Rütti, M.F., Ernst, D., Saely, C.H., Rein, P., Drexel, H., Porretta-Serapiglia, C., Lauria, G., Bianchi, R., von Eckardstein, A., and Hornemann, T. (2012). Plasma deoxysphingolipids: a novel class of biomarkers for the metabolic syndrome? Diabetologia *55*, 421–431.
40. Lone, M.A., Santos, T., Alecu, I., Silva, L.C., and Hornemann, T. (2019). 1-Deoxysphingolipids. Biochim. Biophys. Acta. Mol. Cell Biol. Lipids *1864*, 512–521.
41. Zuellig, R.A., Hornemann, T., Othman, A., Hehl, A.B., Bode, H., Güntert, T., Ogunshola, O.O., Saponara, E., Grabliauskaite, K., Jang, J.H., et al. (2014). Deoxysphingolipids, novel biomarkers for type 2 diabetes, are cytotoxic for insulin-producing cells. Diabetes *63*, 1326–1339.
42. Tran, D., Myers, S., McGowan, C., Henstridge, D., Eri, R., Sonda, S., and Caruso, V. (2021). 1-Deoxysphingolipids, Early Predictors of Type 2 Diabetes, Compromise the Functionality of Skeletal Myoblasts. Front. Endocrinol. *12*, 772925.
43. Tang, W., Yuan, J., Chen, X., Gu, X., Luo, K., Li, J., Wan, B., Wang, Y., and Yu, L. (2006). Identification of a novel human lysophosphatidic acid acyltransferase, LPAAT-theta, which activates mTOR pathway. J. Biochem. Mol. Biol. *39*, 626–635.
44. Huang, Y., Hu, K., Lin, S., and Lin, X. (2022). Glycerol-3-phosphate acyltransferases and metabolic syndrome: recent advances and future perspectives. Expet Rev. Mol. Med. *24*, e30.
45. Shan, D., Li, J.L., Wu, L., Li, D., Hurov, J., Tobin, J.F., Gimeno, R.E., and Cao, J. (2010). GPAT3 and GPAT4 are regulated by insulin-stimulated phosphorylation and play distinct roles in adipogenesis. J. Lipid Res. *51*, 1971–1981.
46. Lauber, C., Gerl, M.J., Klose, C., Ottosson, F., Melander, O., and Simons, K. (2022). Lipidomic risk scores are independent of polygenic risk scores and can predict incidence of diabetes and cardiovascular disease in a large population cohort. PLoS Biol. *20*, e3001561.
47. Meikle, P.J., Wong, G., Barlow, C.K., Weir, J.M., Greeve, M.A., MacIntosh, G.L., Almasy, L., Comuzzie, A.G., Mahaney, M.C., Kowalczyk, A., et al. (2013). Plasma lipid profiling shows similar associations with prediabetes and type 2 diabetes. PLoS One *8*, e74341.
48. Petrenko, V., Gandasi, N.R., Sage, D., Tengholm, A., Barg, S., and Dibner, C. (2020). In pancreatic islets from type 2 diabetes patients, the dampened circadian oscillators lead to reduced insulin and glucagon exocytosis. Proc. Natl. Acad. Sci. USA *117*, 2484–2495.
49. Sinturel, F., Chera, S., Brulhart-Meynet, M.-C., Montoya, J.P., Lefai, E., Jornayvaz, F.R., D'Angelo, G., Jung, M.K., Pataky, Z., Riezman, H., and Dibner, C. (2023). Alterations of lipid homeostasis in serum and white adipose tissue in morbid obese patients are partly reversed by the bariatric surgery. Preprint at medRxiv.
50. Beyene, H.B., Olshansky, G., T Smith, A.A., Giles, C., Huynh, K., Cinel, M., Mellett, N.A., Cadby, G., Hung, J., Hui, J., et al. (2020). High-coverage plasma lipidomics reveals novel sex-specific lipidomic fingerprints of age and BMI: Evidence from two large population cohort studies. PLoS Biol. *18*, e3000870.

51. Matyash, V., Liebisch, G., Kurzchalia, T.V., Shevchenko, A., and Schwudke, D. (2008). Lipid extraction by methyl-tert-butyl ether for high-throughput lipidomics. J. Lipid Res. *49*, 1137–1146.

52. Clarke, N.G., and Dawson, R.M. (1981). Alkaline O leads to N-transacylation. A new method for the quantitative deacylation of phospholipids. Biochem. J. *195*, 301–306.

53. Vale, G., Martin, S.A., Mitsche, M.A., Thompson, B.M., Eckert, K.M., and McDonald, J.G. (2019). Three-phase liquid extraction: a simple and fast method for lipidomic workflows. J. Lipid Res. *60*, 694–706.

54. Pietiläinen, K.H., Sysi-Aho, M., Rissanen, A., Seppänen-Laakso, T., Yki-Järvinen, H., Kaprio, J., and Oresic, M. (2007). Acquired obesity is associated with changes in the serum lipidomic profile independent of genetic effects–a monozygotic twin study. PLoS One *2*, e218.

55. Hartler, J., Trötzmüller, M., Chitraju, C., Spener, F., Köfeler, H.C., and Thallinger, G.G. (2011). Lipid Data Analyzer: unattended identification and quantitation of lipids in LC-MS data. Bioinformatics *27*, 572–577.

STAR★METHODS

KEY RESOURCES TABLE

REAGENT or RESOURCE	SOURCE	IDENTIFIER
Biological samples		
Plasma and adipose tissue samples from ND and T2D individuals at 4 time points around the clock (cohort 1)	Amsterdam UMC (Stenvers et al., 2019)[17]	Netherlands Trial Registry number: NTR3234
Serum samples from ND and obese T2D individuals (cohort 2)	University Hospital of Geneva (Hannich et al., 2020)[18]	ClinicalTrials.gov Identifier: NCT02384148
Chemicals, peptides, and recombinant proteins		
PC 12:0/12:0	Avanti Polar Lipids Inc.	Cat#850335; CAS: 18194-25-7
PE 17:0/14:1	Avanti Polar Lipids Inc.	Cat#LM-1104; CAS: 958763-89-8
PI 17:0/14:1	Avanti Polar Lipids Inc.	Cat#LM-1504; CAS: 1246304-61-9
PS 17:0/14:1	Avanti Polar Lipids Inc.	Cat#LM-1304; CAS: 1036814-91-1
Cer d18:1/17:0	Avanti Polar Lipids Inc.	Cat#860517; CAS: 67492-16-4
SM d18:1/12:0	Avanti Polar Lipids Inc.	Cat#860583; CAS: 474923-21-2
HexCer d18:1/8:0	Avanti Polar Lipids Inc.	Cat#860540; CAS: 111956-47-9
DoxDHCer m18:0/12:0	Avanti Polar Lipids Inc.	Cat#860460
17:0-17:1-17:0 D5 TG	Avanti Polar Lipids Inc.	Cat#860903; CAS: 958760-74-2
1,3-17:0 D5 DG	Avanti Polar Lipids Inc.	Cat#800854; CAS: 1246523-65-8
N-C12-deoxysphingosine m18:1/12:0	Avanti Polar Lipids Inc.	Cat#860455; CAS:1246298-54-3
MTBE (methyl-*tert*-butyl ether)	Sigma Aldrich	Cat#34875; CAS: 1634-04-4
Methylamine solution(33% in absolute ethanol)	Sigma Aldrich	Cat#534102; CAS: 74-89-5
Chloroform	Acros Organics	Cat#326820010; CAS: 67-66-3
Methanol	Acros Organics	Cat#CAS: 67-56-1
n-butanol	Acros Organics	Cat#CAS: 71363
Ammonium molybdate(VI) tetrahydrate	Acros Organics	Cat#CAS: 12054-85-2
Monopotassium phosphate	Sigma Aldrich	Cat#60229; CAS: 7778-77-0
L-ascorbic acid	Sigma Aldrich	Cat#A92902; CAS: 50-81-7
Perchloric acid 70%	Sigma Aldrich	Cat#244252; CAS: 7601-90-3
Hexane	ThermoFisher Scientific	CAS: 110-54-3
Methyl acetate	Sigma Aldrich	CAS: 79-20-9
Acetonitrile	Sigma Aldrich	CAS: 75-05-8
Deposited data		
Raw sequencing data and supplementary files for rhythmic expression analysis (cohort 1)	(Stenvers et al., 2019)[17]	GEO: GSE104674
Software and algorithms		
TSQ Tune 2.6 SP1 QuickQuan™ Software	ThermoFisher Scientific	Catalog number: IQLAAEGABSFAHQMAPT; https://www.thermofisher.com/order/catalog/product/IQLAAEGABSFAHQMAPT
Xcalibur 4.0 QF2 software	ThermoFisher Scientific	Catalog number: OPTON-30965; https://www.thermofisher.com/order/catalog/product/OPTON-30965
LcmsExplorer	EPFL Lausanne Switzerland	http://lipidomes.epfl.ch/
Lipid Data Analyzer	IGB-TUG Graz University	LDA v. 2.6.3.9; https://www.lipidmaps.org/resources/tools/10?task=4.5
CosinorJ program	(Mannic et al., 2013)[20]	http://bigwww.epfl.ch/algorithms/cosinorj/
LS algorithm	(Glynn et al., 2006)[19]	N/A

(*Continued on next page*)

Continued

REAGENT or RESOURCE	SOURCE	IDENTIFIER
MetaboAnalyst 5.0.	McGill University, Canada	https://www.metaboanalyst.ca/MetaboAnalyst/ModuleView.xhtml
Prism Graph Pad 8.0.	Graphpad	https://www.graphpad.com/
Other		
Precellys 24 tissue homogenizer	Bertin Instruments	https://www.bertin-instruments.com/product/sample-preparation-homogenizers/precellys24-tissue-homogenizer/precellys24-4/
Zirconium oxide beads CK14	Labgene Scientific SA	Cat#BER20305
TSQ Vantage Extended Mass Range Mass Spectrometer	ThermoFisher Scientific	https://assets.thermofisher.com/TFS-Assets/CMD/brochures/TSQ%20Vantage.pdf
Hybrid Orbitrap Elite	Thermo Fisher Scientific	https://assets.thermofisher.com/TFS-Assets/CMD/Specification-Sheets/PS-30229-MS-Orbitrap-Elite-PS30229-EN.pdf
LTQ Tuneplus2.7SP2	ThermoFisher Scientific	http://tools.thermofisher.com/content/sfs/manuals/LTQ-Series-Hardware.pdf

RESOURCE AVAILABILITY

Lead contact

Further information and requests for resources and reagents should be directed to and will be fulfilled by the lead contact, Charna Dibner (Charna.Dibner@unige.ch).

Materials availability

This study did not generate new unique reagents.

Data and code availability

- Lipidomics data supporting the findings of this study are available within the Article and Supplemental Materials. In addition, this paper analyzes existing, publicly available RNA-seq data. These accession numbers for the datasets are listed in the key resources table.
- This paper does not report original code.
- Any additional information required to reanalyze the data reported in this paper is available from the lead contact upon request.

EXPERIMENTAL MODEL AND STUDY PARTICIPANT DETAILS

Study design and patient characteristics

Human cohort 1

Two groups comprising six participants each were enrolled in the human cohort 1: lean ND (control group) and overweight or obese T2D men (T2D group; Table S1). Prior to the sample collection, study participants recorded food intake and sleep times at home for 3 days. Subsequently, an individual *Zeitgeber* time (ZT) 0:00 was determined for each participant by the average wake-up time recorded at baseline (Figure 1A). When participants came to the clinical research unit, they received 3 identical meals per day at evenly spaced fixed time points thus tailored to the individual chronotype of each participant (ZT0:30, ZT6:00 and ZT11:30), starting from lunch on day 1. From the evening of day 2, participants slept undisturbed in darkness (0 lux) during their habitual sleep times. On day 3 at ZT0:00, room lights were turned on at ~150 lux at eye level. Blood and SAT samples were obtained on day 2 at ZT15:30, and on day 3 at ZT0:00, ZT5:30 and ZT11:00, with 15 min delay between blood and SAT sampling (Figure 1A, STAR Methods section and Stenvers et al; [17]). We included six overweight or obese individuals with type 2 diabetes (T2D) according to the 2010 American Diabetes Association (ADA) criteria, BMI 25–40 kg/m^2, male sex assigned at birth, aged 30–75 years old, and using no glucose-lowering drugs other than metformin. Inclusion criteria for the six healthy control participants were: BMI $\leq$25 kg/m^2, male sex assigned at birth and age 30–75 years. Exclusion criteria for both groups were: any acute or chronic disease (other than type 2 diabetes) that impairs food digestion, absorption or metabolism, obstructive sleep apnoea, and shift work or crossing more than one time zone in the month prior to study participation. The study was approved by the Institutional Review Board of the AmsterdamUMC (locationAMC) and performed according to the Declaration of Helsinki of October 2004. The study was registered at the Netherlands Trial Registry (number NTR3234) and was performed between February 2012 and March 2013 at the Department of Endocrinology and Metabolism of the Amsterdam UMC. All the participants gave informed consent.

Human cohort 2

We included thirty-two subjects who all gave informed consent to participate to the study. The study had ethics committee approval (CER11-015, ClinicalTrials.gov Identifier: NCT02384148). Exclusion criteria were T1D or LADA, steroid-induced diabetes, post-transplant diabetes, hepatitis, corticosteroid therapy, active neoplasia and ongoing shift work. The participants in the non-diabetic (ND) control and obese T2D groups were age- and sex-matched (according to the sex assigned at birth) (Table S3).

METHOD DETAILS

Study design, blood and tissue sampling

Cohort 1

For a detailed description of the study protocol, refer to.[17] In brief, at baseline, participants recorded food intake and sleep times at home for 3 days (Figure 1A). Subsequently, participants visited the clinical research unit on the morning of day 1. For each participant, an individual *Zeitgeber* time (ZT) 0:00 was determined by the average wake-up time from the baseline sleep log. The individuals with type 2 diabetes were instructed to stop metformin use from 2 days prior to the measurements until study end (a total of 5 days). We provided participants with three identical liquid meals (Ensure Plus [6.3 kJ/mL, 54% energy from carbohydrates, 29% from fat and 17% from protein; Abbott Nutrition, Columbus, OH, USA]) per day at evenly spaced fixed time points (ZT0:30, ZT6:00 and ZT11:30), starting from lunch on day 1. Daily energy intake was set at 105 kJ/kg body weight. Participants returned home and then came back to the clinical research unit on the evening of day 2. Participants slept undisturbed in darkness (0 lux) during their habitual sleep times. On day 3 at ZT0:00, room lights were turned on at ~150 lux at eye level; participants remained in a semi-recumbent position. Superficial subcutaneous adipose tissue samples were obtained by vacuum suction with a 15-gauge needle, from the four peri-umbilical quadrants, in a random order, on day 2 at ZT15:30, and on day 3 at ZT0:15, ZT5:45 and ZT11:15. Frequent blood samples were obtained, and samples from ZT15:30, ZT0:00, ZT5:30 and ZT11:00 were used for lipidomic analysis. Blood plasma was separated from the cells by centrifugation.

Cohort 2

The participants were asked to follow a moderate diet without excess fat or alcohol intake, 24 h prior to the testing day. They filled out the Munich Chronotype Questionnaire (MCTQ), allowing recording of sleep onset time and calculation of sleep duration. Blood samples for all study participants were collected between 8 and 10 a.m., following overnight fasting from 10 p.m. onwards. Serum was immediately prepared from blood samples by centrifugation (10 min, 1650 g, 4°C) and stored at −80°C until lipid extraction and analysis.

Blood measurements

Cohort 1

Plasma glucose concentrations were assessed with the glucose oxidation method with a Biosen glucose analyzer (EKF Diagnostics, Barleben, Germany). Plasma cholesterol and lipids were measured with a Cobas 8000 modular analyzer (Roche Diagnostics, Rotkreuz, Switzerland) and plasma insulin using a chemiluminescent immunometric assay on an Immulite 2000 system (Siemens, Breda, the Netherlands).

Cohort 2

Blood samples were collected in clot-activator vacutainers and immediately analyzed by the Geneva University Hospital laboratory for insulin, blood glucose, HbA_{1c} and total lipid measurements (reported in Table S3 and in Hannich et al; [18]).

Materials for lipid extraction

Synthetic lipid standards [PC 12:0/12:0 (850335), PE 17:0/14:1 (LM-1104), PI 17:0/14:1 (LM-1504), PS 17:0/14:1 (LM-1304), Cer d18:1/17:0 (860517), SM d18:1/12:0 (860583), HexCer d18:1/8:0 (860540), DoxDHCer m18:0/12:0 (860460), 17:0-17:1-17:0 D5 TG (860903), 1,3-17:0 D5 DG (800854) and N-C12-deoxysphingosine m18:1/12:0 (860455)] were from Avanti Polar Lipids Inc. MTBE (methyl-*tert*-butyl ether) and methylamine (33% in absolute ethanol) were purchased from Sigma Aldrich. Chloroform, methanol, n-butanol and ammonium molybdate were from Acros Organics. LC-MS grade methanol, water and ammonium acetate were from Fluka. HPLC-grade chloroform was purchased from Acros Organics. Monopotassium phosphate, L-ascorbic acid, 70% perchloric acid, hexane, methyl acetate and acetonitrile were from Merck.

Serum lipid extraction procedure

Serum lipid extracts were prepared using a modified MTBE extraction protocol with addition of internal lipid standards.[18,51] Briefly, 100 μL serum was used, 360 μL methanol and a mix of internal standards were added (400 pmol PC 12:0/12:0, 1000 pmol PE 17:0/14:1, 1000 pmol PI 17:0/14:1, 3300 pmol PS 17:0/14:1, 2500 pmol SM d18:1/12:0, 500 pmol Cer d18:1/17:0 and 100 pmol HexCer d18:1/8:0). After addition of 1.2 mL of MTBE (methyl *tert*-butyl ether), samples were placed for 10 min on a multitube vortexer at 4°C followed by incubation for 1 h at room temperature (RT) on a shaker. Phase separation was induced by addition of 200 μL MS-grade water. After 10 min at RT, samples were centrifuged at 1000 *g* for 10 min. The upper (organic) phase was transferred into a 13 mm glass tube and the lower phase was re-extracted with 400 μL artificial upper phase [MTBE/methanol/H_2O (10:3:1.5, v/v/v)]. The combined organic phases were dried in a vacuum concentrator (CentriVap, Labconco). Lipid extracts derived from MTBE extraction were

resuspended in 750 μL chloroform: methanol (1:1), sonicated and vortexed. Resuspended lipids were divided in 3 aliquots. One aliquot was used for glycerophospholipid analysis, a second one for phosphorus assay, and the third aliquot was treated by mild alkaline hydrolysis to enrich for sphingolipids, according to the method by Clarke.[52] Briefly, 1 mL freshly prepared monomethylamine reagent [methylamine/H_2O/n-butanol/methanol (5:3:1:4, (v/v/v/v)] was added to the dried lipid extract and then incubated at 53°C for 1 h in a water bath. Lipids were cooled to RT and then dried. For desalting, the dried lipid extract was resuspended in 300 μL water-saturated n-butanol and then extracted with 150 μL H_2O. The organic phase was collected, and the aqueous phase was re-extracted twice with 300 μL water-saturated n-butanol. The organic phases were pooled and dried in a vacuum concentrator.

SAT lipid extraction procedure

SAT lipid extracts were prepared using a modified 3 Phase Extraction Method[53] with addition of internal lipid standards. In addition of the lipid internal standards used for the serum lipid extraction, SAT samples from cohort 1, were supplemented with 1000 pmol of N-C12-deoxysphingosine, 1000 pmol 1,3-17:0 D5 DG and 1000 pmol 17:0-17:1-17:0 D5 TG. Briefly, 30 mg of tissue were homogenized in N_2-cold condition (Precellys24 Bertin Instruments) in presence of zirconium oxide beads CK14 (Labgene Scientific) and 200 μL methanol:dichloromethane solution (1:2). After addition of 1 mL of hexane, 1 mL of methyl acetate and 0.75 mL of acetonitrile, samples were vortexed at room temperature and centrifuged at 2000 g for 5 min, resulting in the separation of three distinct phases. The upper organic phase was collected and neutral lipid extracts were dried in a vacuum concentrator. The middle layer was re-extracted with 1 mL of hexane and the bottom phase, containing the polar lipids, was collected and dried in a vacuum concentrator. Polar lipid extracts were resuspended in 550 μL chloroforme:methanol (1:1) and divided in 2 aliquots. One aliquot was used for phosphorus assay, and the second one was treated by mild alkaline hydrolysis to enrich for sphingolipids as described above.

Determination of total phosphorus

One hundred μL of the total lipid extract, resuspended in chloroform/methanol (1:1), were placed into 13 mm disposable pyrex tubes and dried in a vacuum concentrator. Zero, 2, 5, 10, 20 μL of a 3 mmol/L KH_2PO_4 standard solution were placed into separate pyrex tubes. To each tube, distilled water was added to reach 20 μL of aqueous solution. After addition of 140 μL 70% perchloric acid, samples were heated at 180°C for 1 h in a chemical hood. Then, 800 μL of a freshly prepared solution of water, ammonium molybdate (100 mg/8 mL H_2O) and ascorbic acid (100 mg/6 mL H_2O) in a ratio of 5:2:1 (v/v/v) were added. Tubes were heated at 100°C for 5 min with a marble on each tube to prevent evaporation. Tubes were cooled at RT for 5 min. One hundred μL of each sample was then transferred into a 96-well microplate and the absorbance at 820 nm was measured.

Phospho- and sphingolipid analysis by MS

Mass spectrometry analysis for the quantification of phospho- and sphingolipid species was performed using multiple reaction monitoring on a TSQ Vantage Extended Mass Range Mass Spectrometer (ThermoFisher Scientific), equipped with a robotic nanoflow ion source (Triversa Nanomate, Advion Biosciences) as previously described.[18] Optimized fragmentation was generated using appropriate collision energies and s-lens values for each lipid class. Mass spectrometry data were acquired with TSQ Tune 2.6 SP1 and treated with Xcalibur 4.0 QF2 software (ThermoFisher Scientific). Lipid quantification was carried out using an analysis platform for lipidomics data hosted at EPFL Lausanne Switzerland http://lipidomes.epfl.ch/. Quantification procedure was described in Pietiläinen et al.[54] Dried lipid extracts were resuspended in 250 μL MS-grade chloroform/methanol (1:1) and further diluted in either chloroform/methanol (1:2) plus 5 mmol/L ammonium acetate (negative ion mode) or in chloroform/methanol/H_2O (2:7:1) plus 5 mmol/L ammonium acetate (positive ion mode).

TAG, DAG and Deoxysphingolipid analysis by LC-MS

The detection of 1-deoxyceramides in the samples of cohort 2 has been described in Hannich et al.[18] The 1-deoxyceramide amounts present in the SAT samples of the cohort 1 were normalized and calibrated using the total phosphate content and the integrated signal of the spiked N-C12-deoxysphingosine standard. The tri- and di-acylglycerols amounts present in the neutral fraction of the SAT samples were normalized and calibrated using the total phosphate content and the integrated signal of the spiked standard 1,3-17:0 D5 DG and 17:0-17:1-17:0 D5 TG. Two nanomole of total phosphate content were injected on a HILIC column, diluted in chloroform:methanol 1:2 (v/v). Data were acquired in full-scan mode at high resolution on a hybrid Orbitrap Elite (Thermo Fisher Scientific, Bremen, Germany). using LTQ Tuneplus2.7SP2 and treated with Xcalibur 4.0 QF2 (Thermo Fisher Scientific). Lipid identification was carried out with Lipid Data Analyzer (LDA v. 2.6.3.9, IGB-TUG Graz University),[55] and LcmsExplorer hosted at EPFL Lausanne Switzerland https://lcmsexplorer.epfl.ch. Peaks were identified by their respective retention time, *m/z* and intensity. Instruments were calibrated to ensure a mass accuracy lower than 0.6 ppm in positive mode.

QUANTIFICATION AND STATISTICAL ANALYSIS

Lipid concentrations were calculated relative to the relevant internal standards and normalized to the total phosphate content of each total lipid extract for both tissue and serum samples. Lipid concentrations were not corrected for class II isotopic overlaps for the analysis of lipid degree of unsaturation. For comparison between different lipids samples, relative lipid concentrations were normalized to the total lipid content of each lipid extract (mol %). For temporal analysis, normalized lipid values were z-scored within

subjects. To identify rhythmic variations within the lipidomic dataset, normalized lipid values were further analyzed using the CosinorJ program and the LS algorithm, both allowing to analyze datasets comprising uneven intervals of time between the samplings. For CosinorJ, the period width was set to fit a time frame of 20–28 h and a χ^2 value of $\leq$0.05 was considered statistically significant. For the LS algorithm the top 50 lipids, and the top 10 lipid classes respectively, were considered. For the lipids analyzed by LC-MS, we took into account only the top 10 TAGs and DAGs, and the top 5 DeoxCer species for the subsequent analyses. We next conducted Venn analyses combining both algorithms (Figure 4C). Lipid metabolites and lipid classes commonly identified as rhythmic by these two methods were considered significantly rhythmic, corresponding statistical values are reported in the Table S6. Additional data processing (filtering, normalization, transformation, scaling), statistical analyses and data plotting were performed using MetaboAnalyst 5.0. [91] and Prism Graph Pad 8.0. Statistical tests used for comparison between groups are indicated in the figure legends. Differences were considered significant for $p \leq 0.05$ (*), $p \leq 0.01$ (**) and $p \leq 0.001$ (***). To determine the clustering, k-NN (nearest neighbors with k clusters) was applied to the phases and amplitudes in polar coordinates of all circadian signals for k = 1, 2, and 3 clusters.

ADDITIONAL RESOURCES

The cohort 1 study was registered at the Netherlands Trial Registry (number NTR3234). The cohort 2 study had local ethics committee approval (CER11-015) and was registered at ClinicalTrials.gov (Identifier: NCT02384148).